ANALYSIS OF THE NEUTRONIC BEHAVIOR

OF THE

NUCLEAR ENGINEERING TEACHING LABORATORY REACTOR

AT

THE UNIVERSITY OF TEXAS

Submitted By:

Radiation Center
Oregon State University
Corvallis, Oregon

December 2019

Table of Contents

List of Figures

List of Tables

1. Introduction

This report contains the results of investigation into the neutronic behavior of the Nuclear Engineering Teaching Laboratory reactor (NETL) at the University of Texas Austin. The objectives of this study were to: 1) create a model of the NETL to study the neutronic characteristics, and 2) demonstrate acceptable reactor performance and safety margins for the NETL core under normal conditions.

2. Summary and Conclusions of Principal Safety Considerations

The conclusion of this investigation is that the MCNP model does an acceptable job of predicting behavior of the NETL core. As such, the results suggest that the current NETL core can be safely operated within the parameters set forth in the technical specifications. Discussion and specifics of the analysis are located in the following sections. The final sections of this analysis provide suggestions for a limiting core configuration.

3. Reactor Fuel

The fuel utilized in the NETL is standard TRIGA® fuel manufactured by General Atomics. The use of low-enriched uranium/zirconium hydride fuels in TRIGA® reactors has been previously addressed in NUREG-1282 [1]. This document reviews the characteristics such as size, shape, material composition, dissociation pressure, hydrogen migration, hydrogen retention, density, thermal conductivity, volumetric specific heat, chemical reactivity, irradiation effects, prompt-temperature coefficient of reactivity and fission product retention. The conclusion of NUREG-1282 is that TRIGA® fuel, including the fuel utilized in the NETL, is acceptable for use in reactors designed for such fuel.

The design of standard stainless steel clad fuel utilized in the NETL is shown in Figure 1. Stainless steel clad elements used at NETL all have fuel alloy length of 38.1 cm. The characteristics of standard fuel elements are shown in Table 1.

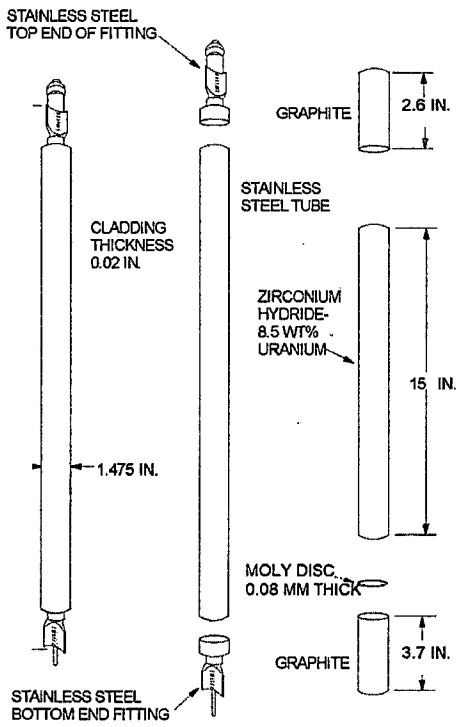

Figure 1 – TRIGA® Stainless Steel Clad Fuel Element Design used in the NETL Core

Table 1 – Characteristics of Stainless Steel Clad Fuel Elements

Uranium content [mass %]	8.5
BOL ^{235}U enrichment [mass % U]	19.75
Original uranium mass [gm]	37
Zirconium rod diameter [in]	0.25
Fuel meat outer diameter [in]	1.435
Cladding outer diameter [in]	1.475
Cladding material	Type 304 SS
Cladding thickness [in]	0.020
Fuel meat length [in]	15
Graphite slug outer diameter [in]	1.43
Upper graphite slug length [in]	2.6
Lower graphite slug length [in]	3.7
Molybdenum disc thickness [mm]	0.8

4. Reactor Core

The NETL core is a seven-ringed hexagonal grid array (labeled A through G) with 121 positions mostly composed of stainless-steel-clad standard TRIGA® fuel elements. The current core configuration contains 113 fuel elements (including three fuel-followed control rods, i.e. FFCRs). The core also contains an air-followed transient rod in C-1, a central thimble in A-1, several non-

fueled locations that allow for a larger irradiation facility (in positions E-11, F-13 and F-14), a startup source in G-32, and a pneumatic transfer (Rabbit) irradiation facility in G-34, and an empty position G-26. The reactor is controlled by three electromagnetic control rods (Shim I, located in D-6; Shim II, located in D-14; and Regulating, located in C-7) and a pneumatic air-followed control rod (Transient, located in C-1), which utilize borated graphite (B_4C) as a neutron poison. Fuel temperature is measured by an instrumented fuel element (IFE) located in B-3. The current core configuration is shown in Figure 2.

Figure 2 – Schematic Illustration of the NETL Showing the Current Core Configuration

Detailed neutronic analyses of the NETL core were undertaken using MCNP6.2 [2]. MCNP6.2 is a general purpose Monte Carlo transport code which permits detailed neutronic calculations of complex 3-dimensional systems. It is well suited to explicitly handle the material and geometric heterogeneities present in the NETL core. The original input deck for the NETL model was developed at UT Austin and modified by Oregon State University. Facility drawings provided by the manufacturer at the time of construction of the facility were used to define the geometry of the core and surrounding structures. The geometry of the stainless steel clad fuel elements and control rods were based upon the manufacturing drawings. Representative cross-sectional views of the MCNP model (of the initial core loading) are shown in Figure 3.

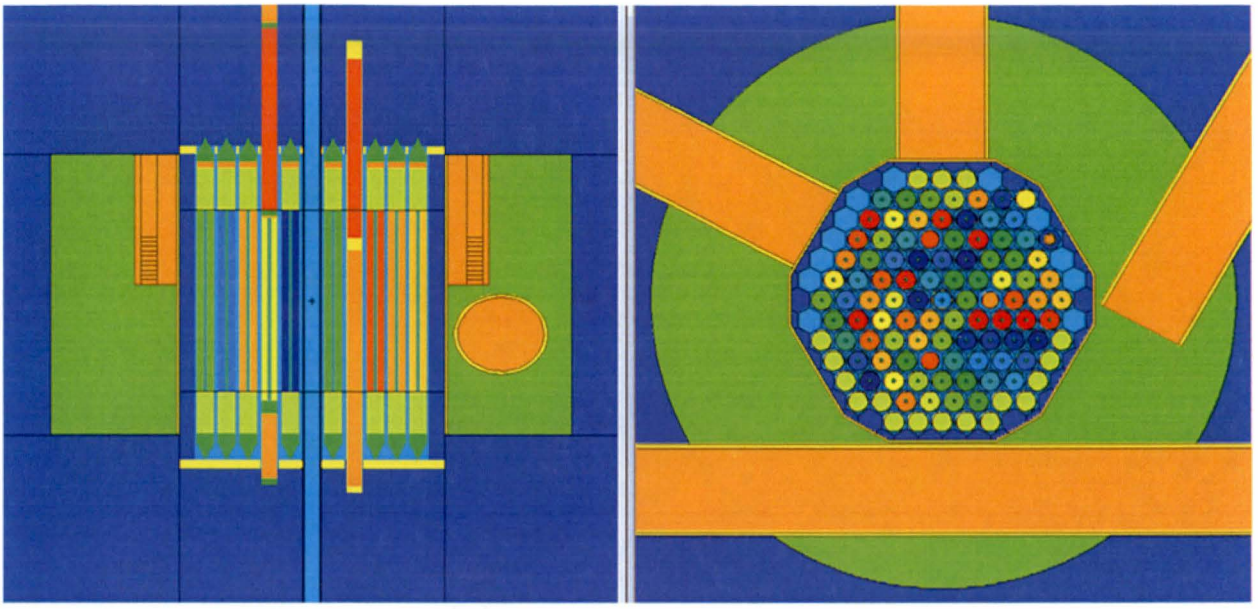

Figure 3 – Horizontal and Vertical Cross-sections of the NETL MCNP Model at BOL

The NETL reactor initially achieved criticality in March of 1992, however all of the fuel (except for the fresh FFCRs) was previously used at other facilities. Most of it came from a previous reactor on campus at Taylor Hall, but there were other sources as well. This made the beginning-of-life (BOL) fuel isotopic determination difficult. UT Austin performed a SCALE analysis to burn the fuel in conjunction with the given burnup records. The SCALE outputs were used to create BOL fuel isotopics for the MCNP runs.

5. Model Bias

Using critical rod height data from the first few months of NETL operation, a series of MCNP analyses based upon various critical rod heights were performed to determine the bias of the model. This bias represents such things as differences in material properties that are difficult to determine or unknown (i.e., exact composition of individual fuel meats and trace elements contained therein) or applicability of cross section data sets used to model the reactor (i.e., interpolation between temperatures). As a result, the validation of the model was based upon the ability of the code to accurately predict criticality as compared with measurements made on the reactor in early 1992.

A criticality calculation was performed using cold clean critical core configuration information from 3/23/1992. The k-effective of this configuration was 0.99393 ± 0.00013, or -\$0.87 ± \$0.04. Eighty different critical core configurations were then analyzed to determine how they bounded

around the bias of this initial critical configuration. Figure 4 shows these 80 configurations with respect to the bias run. All of these kcode calculations utilized 500,000 neutrons per cycle for 200 total cycles (175 active cycles).

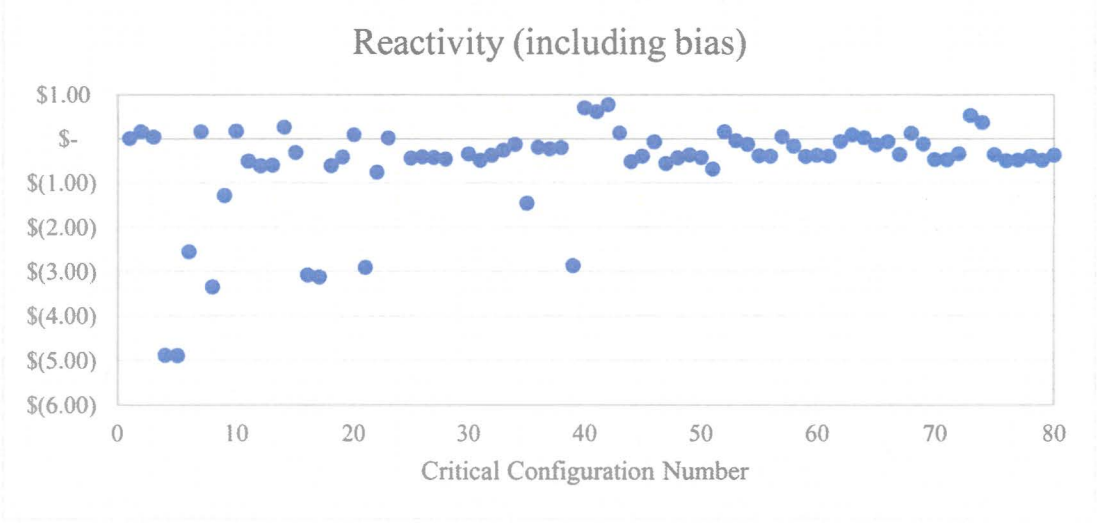

Figure 4 – Reactivity (including bias) of 80 Different BOL Critical Core Configurations

There appears to be significant deviation in the first 40 configurations. Note that most of these configurations are at low power but some are at high power. Most of the configurations with significant deviation are the high power runs, which would indicate that either the model is inaccurate or there is evidence of another problem. If the first 44 runs are ignored (if runs after 5/5/92 are observed), the data looks more accurate (see Figure 5), with an average of -$0.23.

Note that these latter 36 configurations include some full power operations (cases #70-72, 76, 78 and 80). There is only one outlier over ±$0.60 (case #51), which would indicate that there were inconsistencies between high power operations during the first few months of operation. Other evidence, such as lower-than-expected fuel temperatures at these supposed high-power levels, would also indicate that something was inconsistent during the first few months of operation.

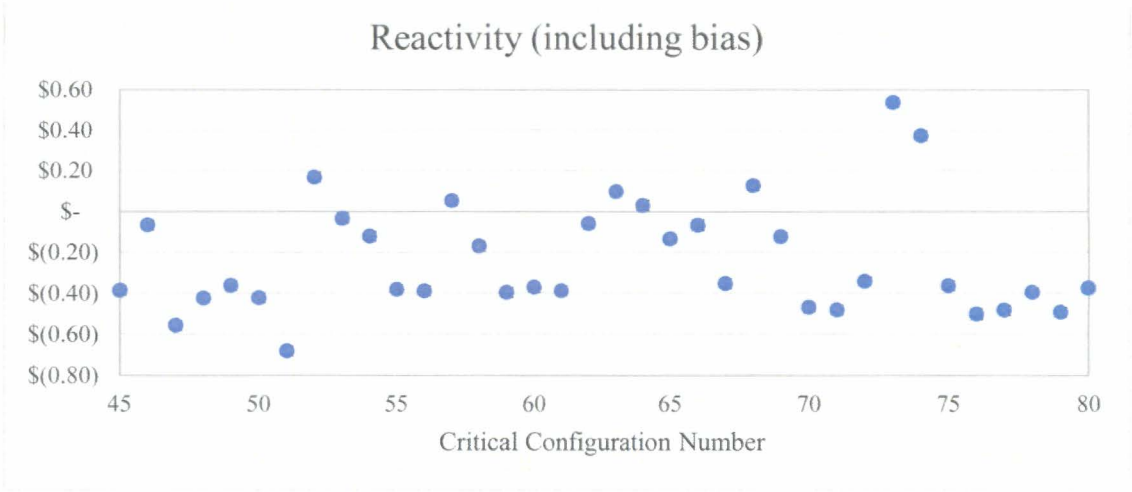

Figure 5 – Reactivity (including bias) of 36 Different BOL Critical Core Configurations

Thus the model bias that will be used for this study is -$1.10 (the -$0.23 bias plus -$0.87 bias). This bias represents such things as differences in material properties that are difficult to determine or unknown (i.e., lack of manufacturer mass spectroscopy data on the exact composition of individual fuel meats and trace elements contained therein) or applicability of cross section data sets used to model the reactor (i.e., interpolation between temperatures). A large source of error is the uncertainty of the contents of the BOL fuel meats, as all of the fuel (except for the FFCRs) was previously irradiated. Without knowing the exact burnup and previous grid location of these elements, it is nearly impossible to accurately determine their fuel compositions. This bias will be used to determine reactivity values in the following sections.

6. Burnup Calculations

After performing the initial model bias calculations, a series of MCNP BURN calculations were performed to burn the NETL fuel to its current core configuration which was established in February 2018. This was a very detailed process as NETL is a very active facility and experienced many different core configurations. Using the fuel move logs, it was determined that there were 18 significant different core configurations that needed to be modeled (see Table 2). Each burnup step involved the fuel burnup for the specified amount of MW-days, parsing of the output fuel isotopics, then subsequent core model reconfiguration.

Table 2 – Summary of Burnup Steps

Burnup Step	From	To	MW-days	Total MW-days	FEs	Note
1	3/19/1992	10/12/1995	9.201	9.201	87	Initial Fuel Load
2	10/12/1995	1/20/1998	5.276	14.477	87	New IFE
3	1/20/1998	6/19/1998	2.789	17.266	87	Fuel Swapped Out/Add Rabbit
4	6/19/1998	3/4/1999	6.376	23.642	87	New IFE
5	3/4/1999	11/12/1999	7.671	31.313	90	Add 3 Fuel Elements
6	4/6/2000	6/29/2000	3.444	34.757	89	Core Reload
7	6/29/2000	1/29/2001	1.919	36.676	92	3L Experiment
8	1/29/2001	7/30/2001	9.138	45.814	92	3L Experiment with New IFE
9	7/30/2001	7/22/2002	21.508	67.322	95	Add 3 Fuel Elements
10	7/22/2002	11/13/2002	13.966	81.288	95	Fuel Shuffle
11	11/13/2002	4/1/2004	24.933	106.221	103	Add 8 New Fuel Elements
12	7/26/2004	7/13/2005	15.71	121.931	102	3L Experiment Core Reload
13	7/13/2005	7/11/2006	22.983	144.914	104	Add 2 Fuel Elements
14	7/11/2006	7/24/2007	41.732	186.646	104	Fuel Shuffle
15	7/24/2007	6/12/2008	18.347	204.993	108	Add 4 Fuel Elements
16	6/12/2008	6/24/2010	21.288	226.281	110	7L Experiment
17	6/24/2010	1/15/2016	73.587	299.868	114	Remove 7L Experiment
18	1/15/2016	2/22/2018	38.026	337.894	114	New IFE

7. Current Core Configuration

Once the burnup calculations were complete, the core was reconfigured to the current core configuration (as of 2/22/2018, see Figure 6). The next series of calculations were then performed to determine various neutronic characteristics of the NETL.

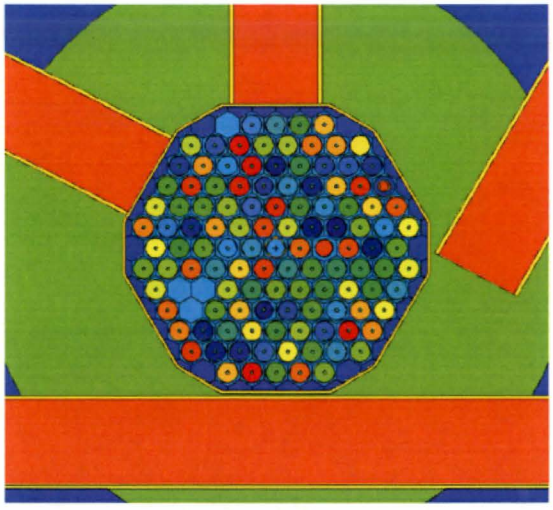

Figure 6 – Vertical Cross-section of Current Core Configuration MCNP Model

Core Power Distribution

F4 flux tallies were used to determine the power-per-element. The tallies output as a fluence per fission neutron. These units were converted to power density (W/cm^3) which were then converted to power-per-element. The individual power-per-element values (in kW) are shown in Figure 7.

								G26	Empty	G27	5.91	G28	5.77	G29	5.7	G30	14.1															
				G24	5.276	F21	7	F22	7.82	F23	8.12	F24	8.2	F25	7.55	F26	6.8	G32	Source													
			G23	5.643	F20	7.553	E17	9.238	E18	10.4	E19	10.7	E20	10.4	E21	9.33	F27	7.63	G33	6.49											
		G22	5.92	F19	7.997	E16	10.4	D13	12	D14	11	D15	12.9	D16	12	E22	10.6	F28	8.679	G34	Rabbit										
	G21	5.5	F18	8.017	E15	10.46	D12	12.48	C09	13.9	C10	14.3	C11	14.1	D17	13.5	E23	11.1	F29	8.61	G35	6.6									
G20	5.2	F17	7.23	E14	9.889	D11	12.3	C08	14.1	B05	16	B06	15.8	C12	15.6	D18	13.6	E24	10.9	F30	8.014	G36	5.9								
	F16	6.3	E13	8.636	D10	11.25	C07	11.69	B04	15.9	A01	CT	B01	16.4	C01	Trans	D01	13.1	E01	9.9	F01	7.4									
G18	5.1	F15	7.44	E12	10.86	D09	12.6	C06	13.9	B03	16.3	B02	16.4	C02	14.5	D02	13.6	E02	11.71	F02	8.471	G2	6.1								
	G17	5.8	F14	Empty	F14	Empty	D08	12.51	C05	14.1	C04	15.3	C03	14.2	D03	13.4	E03	11.6	F03	9.18	G3	6.7									
		G16	6.72	F13	Empty	E10	11.3	D07	11.6	D06	11.3	D05	13.4	D04	12.7	E04	11.4	F04	9.329	G4	7.037										
			G15	5.751	F12	7.657	E09	8.959	E08	10.3	E07	11.3	E06	11.2	E05	10.7	F05	8.63	G5	6.76											
				G14	5.104	F11	6.54	F10	7.68	F09	8.57	F08	8.78	F07	8.29	F06	7.56	G6	6.123												
								G12	5.345	G11	5.96	G10	6.32	G9	6.19	G8	5.88														

Figure 7 – Current Core Power-Per-Element (in kW) Distribution at 1.1 MW

The red highlighting indicates the hottest fuel element location, in B-1, with a maximum power of 16.39 kW (at a total maximum core power of 1.1 MW).

Effective Delayed Neutron Fraction and Prompt Neutron Generation Time

MCNP outputs effective delayed neutron fraction (β_{eff}) and prompt neutron lifetime when using the KOPTS card. Nine different MCNP calculations (the same calculations used in the following Core Excess section) were used to determine β_{eff} and prompt neutron lifetime (see Table 3).

Table 3 – β_{eff} and Prompt Neutron Lifetimes for Current Core Configuration

Case	Prompt Neutron Generation Time (s)	Error (s)	β_{eff}
Trans fully in	47.62	7.543	0.00705
Trans fully out	46.868	7.111	0.00716
Reg fully in	48.08	7.824	0.00707
Reg fully out	46.718	6.961	0.00707
Shim I fully in	48.023	7.748	0.00702
Shim I fully out	46.777	6.974	0.00705
Shim II fully in	48.104	7.684	0.00717
Shim II fully out	46.708	7.086	0.00713
All Rods Out	45.824	6.626	0.00720
Average	47.191	7.284	0.00710

The average effective delayed neutron fraction β_{eff} was calculated to be 0.00710 ± 0.00007. This is in reasonable agreement with values predicted in other LEU TRIGA® cores (i.e., Oregon State University $\beta_{eff} = 0.0076$ [3], University of Maryland $\beta_{eff} = 0.007$ [4]) and also the value historically used for the NETL of $\beta_{eff} = 0.007$. The value $\beta_{eff} = 0.007$ will be used to express all dollar values of reactivities in this report.

The average prompt neutron generation time for the cases I Table 3 is 47.191 ± 7.284 seconds.

Core Excess, Control Rod Worth and Shutdown Margin

Nine different MCNP calculations were performed to determine core excess, control rod worth, and shutdown margin. Core excess is calculated as the reactivity of all rods withdrawn from the core. Control rod worths and shutdown margin were calculated by determining a critical state of the reactor with one rod full inserted and the other three rods banked at the same height, then fully withdrawing the previously-inserted rod. The resulting values (with comparison to values measured at NETL) are shown in Table 3.

Table 4 – Current Core Rod Worth Calculations

Case	MCNP k-effective Rod Full-In	MCNP k-effective Rod Full-Out	MCNP Rod Worth	Experimental Reactivity	Difference
Transient	1.00035	1.02354	$3.24	$3.44	-$0.20
Regulating	0.99978	1.02214	$3.13	$3.18	-$0.05
Shim 1	1.00078	1.02248	$3.03	$3.09	-$0.06
Shim 2	1.00014	1.0211	$2.93	$2.94	-$0.01
All Rods Out (Core Excess)	-	1.04118	$6.75	$6.06	$0.69

MCNP appears to accurately calculate the individual rod worths. The Regulating, Shim 1 and Shim 2 rods are all within the margin of error (which is approximately ±$0.06 for each case).

These calculations show a core excess of $6.75 ± $0.03. This is below the technical specification limit of $7.00. The core excess was measured by NETL to be $6.06 on 3/6/18. MCNP appears to have over-estimated core excess by approximately $0.70. This could be due to a variety of reasons, such as only modeling the fuel elements as one single material per element, thus some burnup resolution is lost as the fuel does not burn uniformly throughout.

The technical specification definition of shutdown margin is "the minimum reactivity necessary to provide confidence that the reactor can be made subcritical by means of the control and safety systems starting from any permissible operating condition (the highest worth MOVEABLE EXPERIMENT in its most positive reactive state, each SECURED EXPERIMENT in its most reactive state), with the most reactive rod in its most reactive position, and that the reactor will remain subcritical without further operator action." The most reactive rod is the Transient rod.

Total rod worth minus the Transient rod is \$9.09 ± \$0.06. NRC shutdown margin is this value minus the core excess, which would be \$2.34 ± \$0.06, which is far above the technical specification limit of \$0.29.

Prompt Fuel Temperature Coefficient

The prompt-temperature coefficient associated with the NETL fuel, α_F, was calculated by varying the fuel meat temperature while leaving other core parameters fixed. The MCNP model was used to simulate the reactor with all rods out at 293, 600, 900, 1200 and 2500 K. The prompt-temperature coefficient for the fuel was calculated at the mid-point of the four temperature intervals. The results are shown in Figure 8 and tabulated in Table 5. Results from GA were added to show similarity [5]. The prompt-temperature coefficient is observed to be negative for all evaluated temperature ranges with decreasing magnitude as temperature increases. The coefficient has a value of -1.3¢/°C at 446.8 K, which is similar to the value of -0.01%/°C stated in the original SAR [6].

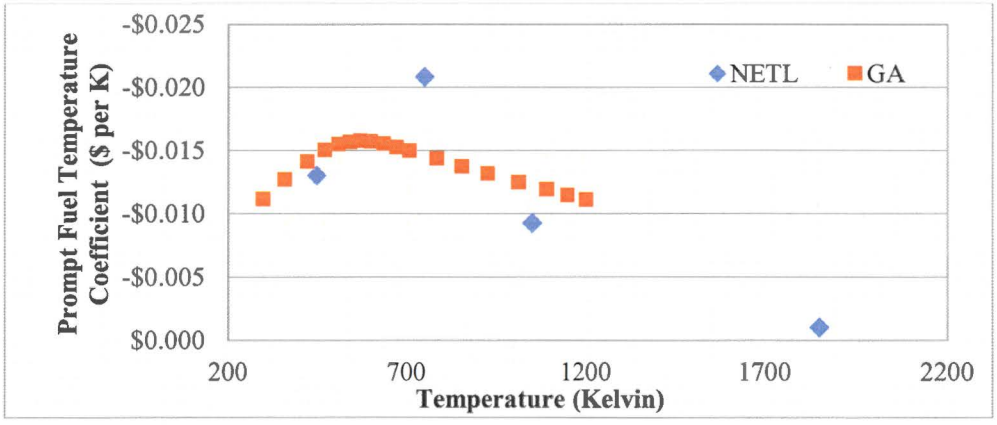

Figure 8 – Current Core Configuration Prompt Temperature Coefficient, α_F, as a Function of Temperature

Table 5 – Current Core Configuration Prompt Temperature Coefficient

Fuel Temperature [K]	Prompt Temperature Coefficient [\$/°C]
446.8	-\$0.0130
750	-\$0.0208
1050	-\$0.0092
1850	-\$0.0010

Moderator Void Coefficient

The moderator void coefficient of reactivity was also determined using the MCNP model. The voiding of the core was introduced by uniformly reducing the density of the liquid moderator in the entire core. The calculation was performed from 0% to 100% voiding at 10% intervals. The void coefficient was negative for every interval and steadily decreased, as can be seen in Figure 9.

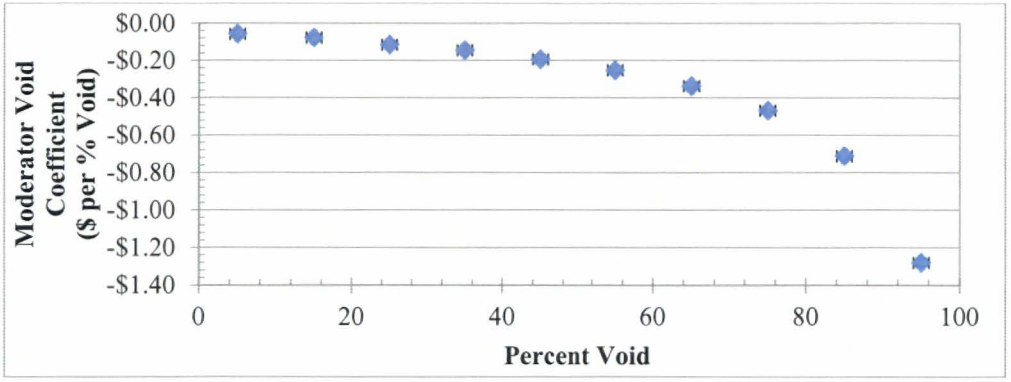

Figure 9 – Current Core Configuration Moderator Void Coefficient

Moderator Temperature Coefficient

The moderator temperature coefficient of reactivity, α_M, was determined by varying the moderator density with respect to temperature within the MCNP model from the expected operating temperature range of 20°C to 50°C (using Engineering Toolbox [7] to determine water density). The results are shown in Figure 10. The moderator temperature coefficient is calculated to be slightly positive from 25°C to 30 °C and from 45 °C to 50 °C, but these changes are less than \$0.01/°C and both points (with 2-sigma error) are bounded around zero. The moderator temperature coefficient appears to be negligible.

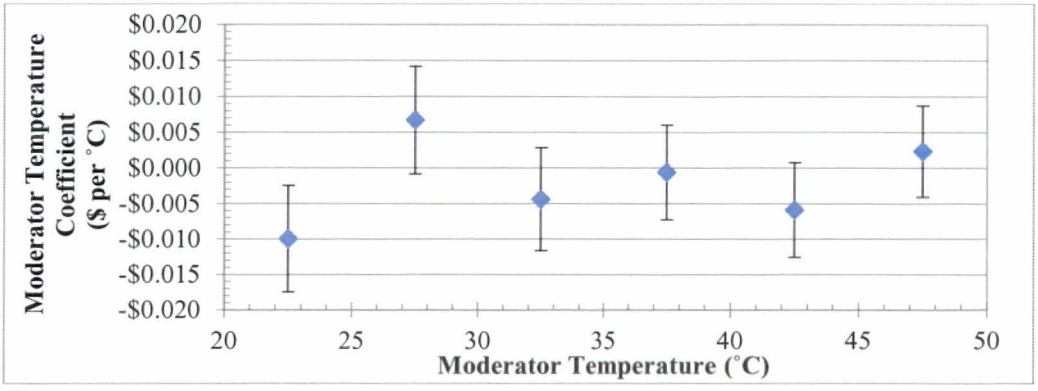

Figure 10 – Current Core Configuration Moderator Temperature Coefficient

Power Coefficient of Reactivity

The power coefficient of reactivity, otherwise known as power defect, is the amount of reactivity required to overcome the temperature feedback during the rise to power. This is modeled by analyzing two MCNP decks that are similar except for the neutron cross-sections used. Two k-effective calculations were performed with all rods out, one using cross sections at 293K (low power) and one using cross sections at 600K (full power). The results are seen in Table 6.

Table 6 – K-Effective Calculations Used to Determine Current Core Power Defect

Case	MCNP k-effective	Standard Deviation	Reactivity	Error (2-sigma)
Low Power	1.04118	0.00012	\$6.75	\$0.03
Full Power	1.01327	0.00010	\$2.94	\$0.03

Power defect is simply the difference in reactivity between these two cases; thus the power defect is \$3.81 ± \$0.05.

8. Limiting Core Configuration

This section will suggest a limiting core configuration that utilizes fresh fuel to improve reactor efficiency while maintaining proper safety margins. The NETL limiting core configuration is a core that completely consists of fresh fuel.

Figure 11 shows the suggested limiting core configuration. For this analysis, it is suggested that the core is loaded with 84 fresh fuel elements (including FFCRs), which will provide just under the license limit of \$7.00 core excess (\$6.93 ± \$0.07). This is comparable to the original 1992 BOL core configuration, which was measured to have a \$6.38 core excess on a core of 87 lightly-irradiated fuel elements. This configuration will provide maximum flux to the beam port facilities while maintaining safety margins.

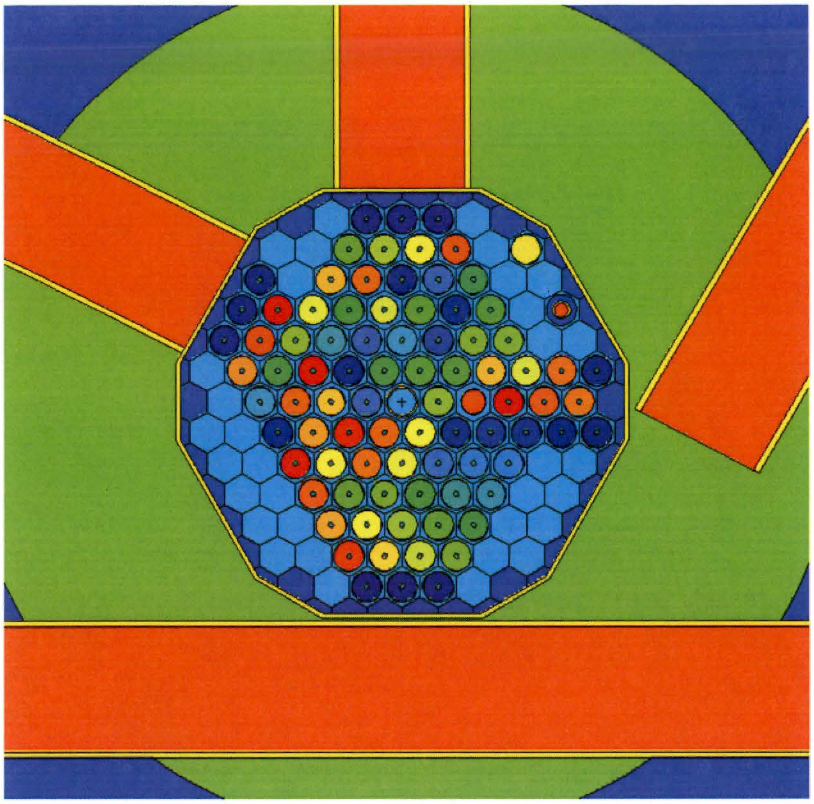

Figure 11 – Vertical Cross-section of Limiting Core Configuration MCNP Model

Core Power Distribution

Figure 12 shows the power-per-element (in kW) in the suggested limiting core configuration.

								G26	Empty	G27	6.21	G28	5.93	G29	5.90	G30	18.01						
				G24	Empty	F21	Empty	F22	10.37	F23	10.17	F24	9.88	F25	9.49	F26	Empty	G32	Source				
			G23	6.74	F20	Empty	E17	13.18	E18	13.64	E19	14.05	E20	12.77	E21	11.52	F27	Empty	G33	Empty			
		G22	5.76	F19	10.65	E16	14.12	D13	16.05	D14	14.99	D15	16.87	D16	14.61	E22	12.74	F28	Empty	G34	Rabbit		
	G21	5.76	F18	9.70	E15	13.76	D12	17.09	C09	19.22	C10	19.62	C11	18.13	D17	15.33	E23	13.08	F29	Empty	G35	Empty	
G20	Empty	F17	9.36	E14	12.68	D11	16.75	C08	19.75	B05	22.14	B06	21.59	C12	18.75	D18	15.70	E24	11.85	F30	8.55	G36	4.72
	F16	Empty	E13	11.45	D10	14.75	C07	15.98	B04	22	A01	CT	B01	21.48	C01	Trans	D01	14.41	E01	9.72	F01	6.43	
G18	Empty	F15	Empty	E12	12.69	D09	15.69	C06	18.87	B03	21.58	B02	21.22	C02	18.52	D02	15.56	E02	11.81	F02	8.53	G2	4.67
	G17	Empty	F14	Empty	E11	Empty	D08	15.35	C05	18.01	C04	18.79	C03	17.52	D03	14.90	E03	12.93	F03	Empty	G3	Empty	
		G16	Empty	F13	Empty	E10	12.46	D07	14.34	D06	13.87	D05	15.90	D04	14.04	E04	12.43	F04	Empty	G4	Empty		
			G15	Empty	F12	Empty	E09	11.06	E08	12.17	E07	13.02	E06	12.02	E05	11.02	F05	Empty	G5	Empty			
				G14	Empty	F11	Empty	F10	8.90	F09	9.20	F08	9.20	F07	8.90	F06	Empty	G6	Empty				
								G12	Empty	G11	5.45	G10	5.45	G9	5.46	G8	Empty						

Figure 12 – Limiting Core Configuration Power-Per-Element Distribution at 1.1 MW

The hottest fuel element in now in location B-5. This makes sense as the core is more shifted to the northwest, which would better centralize the location of the maximum power production around B-5. Also, the hottest power-per-element at 1.1 MW is now 22.14 ± 0.06 kW, which is

higher than the current core hot channel, due to a lower fuel loading concentrating more power at the center of the core.

Effective Delayed Neutron Fraction and Prompt Neutron Generation Time

Once again using the "KOPTS" card and running nine cases, the effective delayed neutron fraction β_{eff} and prompt neutron generation times were calculated

Table 7 – β_{eff} and Prompt Neutron Lifetimes for Limiting Core Configuration

Case	Prompt Neutron Generation Time (s)	Error (s)	β_{eff}
Trans fully in	42.828	5.531	0.00743
Trans fully out	42.721	5.024	0.00725
Reg fully in	43.764	5.502	0.00732
Reg fully out	41.951	4.985	0.00742
Shim I fully in	43.546	5.616	0.00737
Shim I fully out	42.407	5.104	0.00737
Shim II fully in	43.614	5.458	0.00733
Shim II fully out	42.261	5.200	0.00728
All Rods Out	42.024	4.965	0.00742
Average	42.791	5.265	0.00735

The average β_{eff} was calculated to be 0.00735 ± 0.00007. There is a slight increase in β_{eff} compared to the current core configuration, but for consistency, 0.007 will continue to be used to express all dollar values of reactivities in this report.

The average prompt neutron generation time is 42.791 ± 5.265 seconds.

Core Excess, Control Rod Worth, and Shutdown Margin

The same nine MCNP rod worth calculations were performed again for the limiting core configuration: Core excess, shutdown margin, and individual rod worths were calculated from these outputs and the reactivity values (with the bias taken into account) of each of these calculations are shown in Table 7.

Table 8 – Limiting Core Configuration Rod Worth Calculations

Case	MCNP k-effective Rod Full-In	MCNP k-effective Rod Full-Out	MCNP Rod Worth
Transient	0.99886	1.02191	$3.22
Regulating	1.00024	1.03222	$4.43
Shim 1	1.00003	1.02431	$3.39
Shim 2	1.0003	1.02857	$3.93
All Rods Out (Core Excess)	-	1.04257	$6.93

These calculations show a core excess of $6.93 ± $0.07. This is below the technical specification limit of $7.00.

Now the most reactive rod is the Regulating, due to having more fuel near its vicinity and the power shifted to the northwest side of the core. Total rod worth minus the Regulating Rod is $10.53 ± $0.16. NRC shutdown margin is this value minus the core excess, which would be $3.60 ± $0.16, which is still far above the technical specification limit of $0.29.

Prompt Fuel Temperature Coefficient

The results of the limiting core configuration prompt fuel temperature coefficient calculations are shown in Figure 13 and tabulated in Table 9.

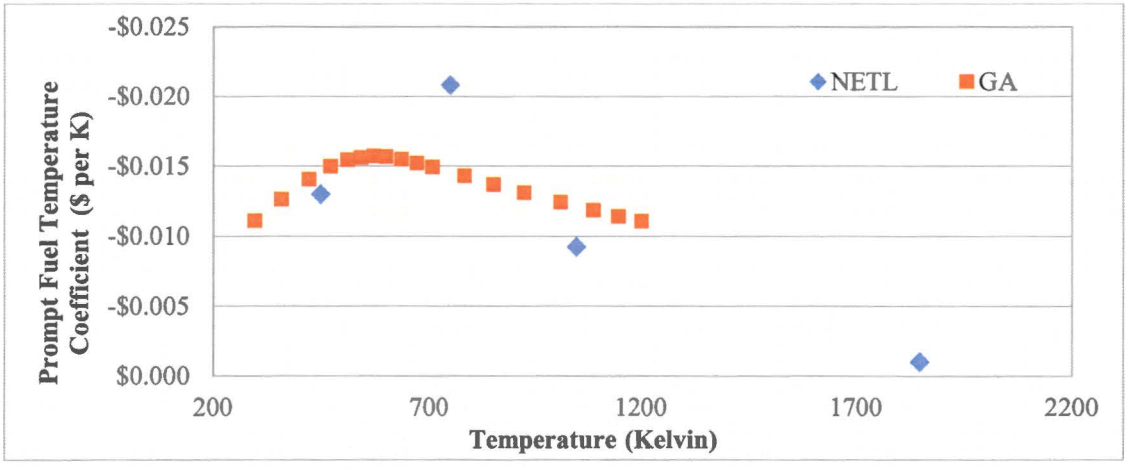

Figure 13 – Limiting Core Configuration Prompt Temperature Coefficient, α_F, as a Function of Temperature

Table 9 – Limiting Core Configuration Prompt Temperature Coefficient

Fuel Temperature [K]	Prompt Temperature Coefficient [$/°C]
446.8	-$0.01302
750	-$0.02081
1050	-$0.00928
1850	-$0.00105

These values are similar to the original BOL coefficients.

Moderator Void Coefficient

Figure 14 shows the moderator void coefficient in the suggested limiting core configuration.

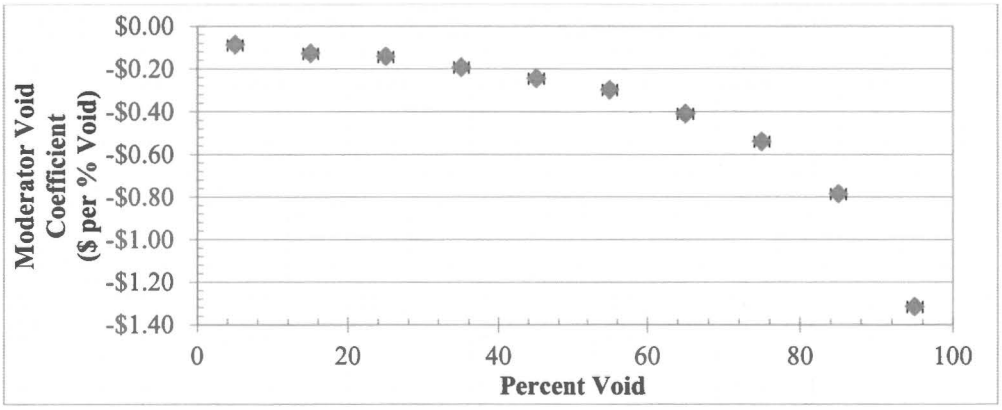

Figure 14 – Limiting Core Configuration Moderator Void Coefficient

The void coefficient was negative for every interval and steadily decreased, similar to the current core configuration. The void coefficient is slightly more negative in the limiting core configuration, likely due to having more moderator in the core configuration.

Moderator Temperature Coefficient

Figure 15 shows the moderator temperature coefficient in the suggested limiting core configuration.

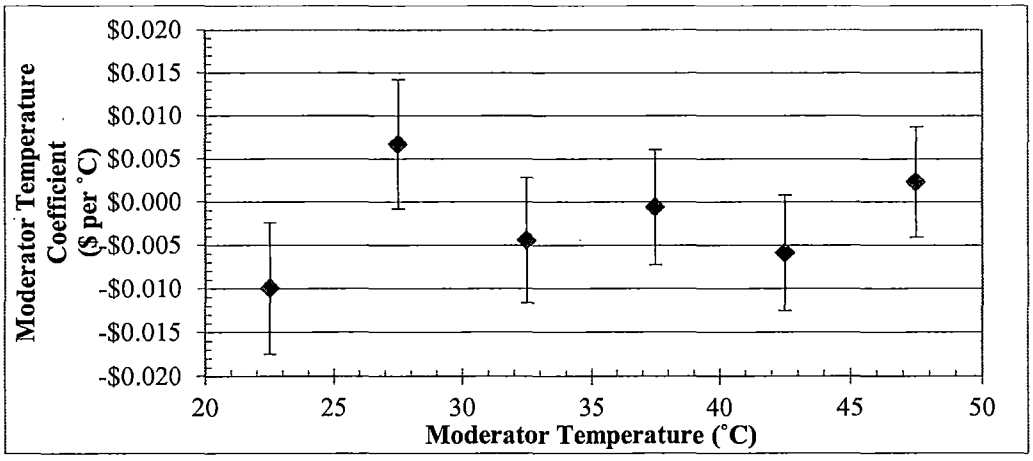

Figure 15 – Limiting Core Configuration Moderator Temperature Coefficient

Once again the moderator temperature coefficient appears to be negligible as it bounds around $0.00 at all observed temperature ranges.

Power Coefficient of Reactivity

The power coefficient of reactivity results are seen in Table 10.

Table 10 – K-Effective Calculations Used to Determine Limiting Core Power Defect

Case	MCNP k-effective	Standard Deviation	Reactivity	Error (2-sigma)
Low Power	1.04231	0.00015	$6.90	$0.04
Full Power	1.01921	0.00010	$3.79	$0.03

Thus the power defect is $3.11 ± $0.05. This is lower than the current core configuration's power defect, likely due to less resistance at the point-of-adding-heat due to the lower amount of zirconium-hydride in the core.

Hot Channel Power Summary

The hot channel in the limiting core configuration was determined to be B-5. An fmesh calculation was performed to analyze a 20 by 20 mesh array to determine axial and radial power distributions. Table 11 summarizes the results of this calculation.

Table 11 – Limiting Core Hot Channel Power Summary

Core Configuration	Hot Rod Location	Hot Rod Thermal Power [kW]	Hot Rod Peak Factor [P_{max}/P_{avg}]	Hot Rod Axial Peak Factor [P_{max}/P_{avg}]	Hot Rod Radial Peak Factor [P_{max}/P_{avg}]	Effective Peak Factor
Limiting Core	B6	22.14	1.691	1.296	1.017	2.229

9. Summary

MCNP6.2 was used to calculate fundamental and operational parameters for the Nuclear Engineering Teaching Laboratory Reactor to demonstrate the reactor's adherence to safety margins in the technical specifications. Values of fundamental parameters agree well with theoretical values. Values of operational parameters agree well with measured values, giving confidence in the model's ability to predict the viability of future core configurations. The results of this study indicate that the NETL can be operated safely within the Technical Specification bounding envelope and that its MCNP model can be used to predict future core configuration changes.

REFERENCES

[1] NUREG-1282, "Safety Evaluation Report on High-Uranium Content, Low-Enriched Uranium-Zirconium Hydride Fuels for TRIGA® Reactors,' USNRC, August 1987.

[2] C.J. Werner, et al., "MCNP6.2 Release Notes", Los Alamos National Laboratory, report LA-UR-18-20808 (2018).

[3] "Safety Analysis Report for the Conversion of the Oregon State University TRIGA® Reactor from HEU to LEU Fuel," Submitted by the Oregon State University TRIGA® Reactor (2007).

[4] "Analysis of the Neutronic Behavior of the Maryland University Training Reactor," Submitted by the Oregon State University Radiation Center to the Department of Energy (July 2017).

[5] GA-7882, Kinetic Behavior of TRIGA® Reactors, General Atomics (1967).

[6] "Safety Analysis Report" Submitted by the University of Texas at Austin Nuclear Engineering Teaching Laboratory (January 2012).

[7] Engineering Toolbox. Web. Accessed May 3rd, 2017.

Link: http://www.engineeringtoolbox.com/water-thermal-properties-d_162.html

THERMAL HYDRAULIC ANALYSIS OF

THE UNIVERSITY OF TEXAS (UT) TRIGA REACTOR

Paul (Michael) Whaley and William S. Charlton
Nuclear Engineering Teaching Laboratory
University of Texas at Austin
Austin, TX 78758

April 15, 2020

1.0 INTRODUCTION

This report documents analysis of the thermal hydraulic characteristics of the UT TRIGA nuclear research reactor in support of renewal of the U.S. Nuclear Regulatory Commission facility operating license. NRC guidance[1] specifies definition of a limiting core configuration (LCC) as the core that would yield the highest power density using the fuel specified for the reactor, with all other core configurations encompassed by safety analysis for the LCC. Coupled analyses for neutronic and thermal hydraulic behavior are used to characterize thermal hydraulic performance of the LCC. This report describes the thermal hydraulic analysis, the neutronic analysis is a separate report[2].

Heat generated by fission in operation of the UT TRIGA reactor is transferred by conduction from the fuel to the cladding. The fuel cladding is the principal safety feature of the TRIGA reactor, preventing radioactive fission products from release that could result in possible hazardous exposure to radiation for facility personnel and the general public. The integrity of the fuel cladding is assured if the fuel temperature remains below specific values (830°C during pulsing[3], 950°C if the cladding temperature is less than 500°C, and 1150°C if the cladding temperature is above 500°C[4]).

Heat is transferred to water [or air in the case of a loss of coolant accident (LOCA)] surrounding the fuel element cladding. The cooling media temperature increase develops buoyancy forces that drive convection flow. Cooling flow is impeded by momentum changes and friction (across the grid plates, fuel element end fittings, and fuel element cladding surfaces). Above a "critical" heat flux (CHF), cooling flow may not be adequate to prevent exceeding the temperature limits, and 'burnout' may occur. The NRC guidance limits the ratio of heat flux to critical heat flux (CHFR) to a value greater than 2.0. A correlation for CHFR applicable to TRIGA reactors has been developed by Bernath[5] and is used in this analysis.

The fuel element in the LCC that operates closest to the limits is the element generating the most power, 'hot channel.' Analysis of the hot channel demonstrates that operation at the maximum licensed power level and within licensed reactivity limits maintains the reactor fuel below the temperature limits, and heat transfer to the surrounding cooling media remains above the CHFR limit.

TRACE (TRAC/RELAP Advanced Computational Engine) is the NRC's flagship thermal-hydraulics analysis tool consolidating and extending the capabilities of NRC's three legacy safety codes: TRAC-P, TRAC-B and RELAP. These codes are designed to perform best-estimate analyses of operational transients and accident scenarios by modeling physical geometry and thermodynamic conditions. TRACE and RELAP were developed for commercial nuclear reactors applications, and RELAP has also been widely used in characterizing non-power/research reactor thermal hydraulic performance. Thermal hydraulic modeling of the hot channel in the UT TRIGA reactor was performed using TRACE.

The hot channel model was developed for TRACE using standard, classical methods applied to the fuel element geometry and fuel element pitch. However, fuel element construction includes complex end fittings not well represented in modeling flow resistance classically, and coefficients characterizing the resistance to

---

[1] NURGE 1537, *Guidelines for Preparing and Reviewing Applications for the Licensing of Non-Power Reactors, Format and Content*

[2] Analysis of the Neutronic Behavior of the Nuclear Engineering Teaching Laboratory at The University of Texas, Radiation Center – Oregon State University

[3] TRD-070-0.1006.05 Rev A, *Pulsing Temperature Limit for TRIGA Fuel* (TRIGA Reactors Division of General Atomics-ESI, 2008)

[4] NUREG/CR-2387 *Credible Accident Analyses for TRIGA and TRIGA-Fueled Reactors* (PNL-4028, April 1962)

[5] ANL RETR TM 07 01, Fundamental Approach to TRIA Steady-State Thermal-Hydraulic CHF Analysis, E. E. Feldman (2007)

cooling flow for the UT TRIGA were therefore developed in the computational fluid dynamics code FLUENT.[6] Data in TRACE output files were parsed to identify maximum fuel temperature and variables used in the Bernath correlation.

TRACE has an internal library of standard material properties relevant to power reactors. The library does not include properties for zirconium and TRIGA fuel; these material characteristics were supplied as manual input. The ratio of the maximum power in the hot channel to average core-wide element power (peaking factor, developed from the neutronics analysis) is used to extend transient calculations from elements generating core average power to calculations for the element generating the maximum power in the core.

The MCNP model developed in the neutronics analysis was used to calculate power generated in each fuel element, fractions and energy of fast and thermal fissions, β_{eff}, and (in an adjoint calculation) delayed neutron precursor constants and the prompt neutron lifetime. An auxiliary program distributed with MCNP (MAKXS) was used to generate neutron interaction cross sections at specific fuel and water temperatures. These cross sections were used in MCNP criticality calculations to develop reactivity temperature-coefficients for TRACE reactivity calculations. The delayed neutron precursor constants were used to develop time-dependent heat generation from fission following shutdown for LOCA analysis. The heat generation from fission product decay for LOCA analysis was developed from the method described in ANSI/ANS-5.1-2014, Decay Heat Power in Light Water Reactors. Heat generated from neutron interaction with fission products was neglected.

The model was used characterize performance of the LCC following validation. Analyses were developed to characterize performance associated with steady-state operation, reactor pulsing, continuous control rod withdrawal transients, and a LOCA. Validation of the modeling was performed by comparing the results of analyses to peak temperatures during steady state operations, and power levels and temperatures that occurred during pulsing operation.

2.0 TRACE MODEL

The TRACE model uses 'break' elements that establish pressure and temperature fluid boundary conditions. Pool water is delivered from break through a 'downcomer' with a horizontal structure connecting the downcomer to the inlet of the fuel element flow channel. The fuel element flow channel discharges to another break. A conceptual diagram of the model is provided in Fig. 1.

2.1 Flow Channel Geometry

The inner diameter of the TRIGA fuel (an annulus filled with a 0.225 in. diameter zirconium rod) is 0.25 in. The outer diameter of the fuel is 1.435 in. There is a small gap between the fuel and the cladding; the radial gap for production elements is estimated to be less than 0.0025 in.[7] and was assumed to be 0.00126 in. for this analysis. The cladding is 0.02 in. thick. The outer diameter of standard TRIGA fuel is nominally 1.475 in. and was modeled as slightly expanded in this analysis to 1.478 (D_F) in order to model the gap, which is a major contributor to temperature elevation in the fuel compared to the cladding. (With cladding 1.475 in. diameter and thickness of 0.02 in., the inner cladding diameter of 1.435 in. does not have a gap between cladding and the 1.435 in. diameter fuel element.) The center-to-center distance to adjacent elements (pitch, P_e) is 1.714 in.

---

[6] (Doctoral Dissertation) Development of thermal Hydraulic Correlations for the University of Texas at Austin TRIGA Reactor Using Computational Fluid Dynamics and In-Core measurements, A. D. Brand (2013), https://repositories.lib.utexas.edu/handle/2152/23039

[7] Fission Product Release from TRIGA-LEU Reactor Fuels, N. L. Baldwin, F. C. Fousheee and J. S. Greenwood (10/1980)

cooling flow for the UT TRIGA were therefore developed in the computational fluid dynamics code FLUENT.[6] Data in TRACE output files were parsed to identify maximum fuel temperature and variables used in the Bernath correlation.

TRACE has an internal library of standard material properties relevant to power reactors. The library does not include properties for zirconium and TRIGA fuel; these material characteristics were supplied as manual input. The ratio of the maximum power in the hot channel to average core-wide element power (peaking factor, developed from the neutronics analysis) is used to extend transient calculations from elements generating core average power to calculations for the element generating the maximum power in the core.

The MCNP model developed in the neutronics analysis was used to calculate power generated in each fuel element, fractions and energy of fast and thermal fissions, β_{eff}, and (in an adjoint calculation) delayed neutron precursor constants and the prompt neutron lifetime. An auxiliary program distributed with MCNP (MAKXS) was used to generate neutron interaction cross sections at specific fuel and water temperatures. These cross sections were used in MCNP criticality calculations to develop reactivity temperature-coefficients for TRACE reactivity calculations. The delayed neutron precursor constants were used to develop time-dependent heat generation from fission following shutdown for LOCA analysis. The heat generation from fission product decay for LOCA analysis was developed from the method described in ANSI/ANS-5.1-2014, Decay Heat Power in Light Water Reactors. Heat generated from neutron interaction with fission products was neglected.

The model was used characterize performance of the LCC following validation. Analyses were developed to characterize performance associated with steady-state operation, reactor pulsing, continuous control rod withdrawal transients, and a LOCA. Validation of the modeling was performed by comparing the results of analyses to peak temperatures during steady state operations, and power levels and temperatures that occurred during pulsing operation.

2.0 TRACE MODEL

The TRACE model uses 'break' elements that establish pressure and temperature fluid boundary conditions. Pool water is delivered from break through a 'downcomer' with a horizontal structure connecting the downcomer to the inlet of the fuel element flow channel. The fuel element flow channel discharges to another break. A conceptual diagram of the model is provided in Fig. 1.

2.1 Flow Channel Geometry

The cooling flow channel is modeled as a heated pipe with thermodynamic characteristics based on physical dimensions and properties of the coolant surrounding the fuel elements. The outer diameter of the fuel element cladding (D_F) is 1.475 in. The cladding is 0.020 in. thick, with a small gap between the inner cladding diameter and the fuel outer diameter. The outer diameter of the fuel is 1.435 in. with an inner diameter of 0.25 in. that is filled with a 0.225 in. diameter zirconium rod. The center-to-center distance to adjacent elements (pitch, P_e) is 1.714 in.

[6] (Doctoral Dissertation) Development of thermal Hydraulic Correlations for the University of Texas at Austin TRIGA Reactor Using Computational Fluid Dynamics and In-Core measurements, A. D. Brand (2013), https://repositories.lib.utexas.edu/handle/2152/23039

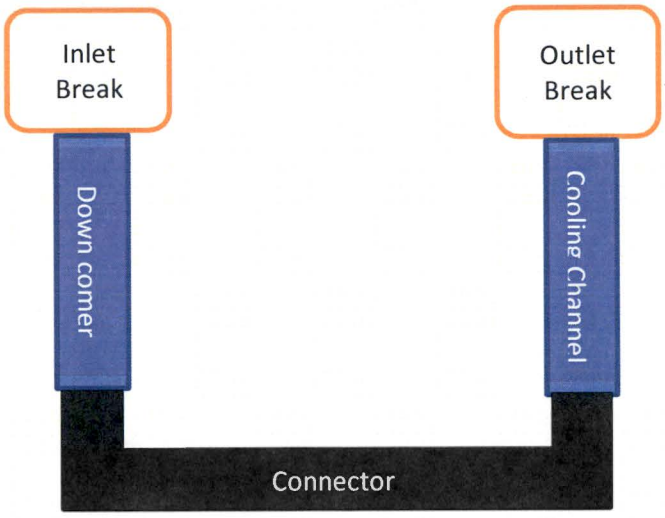

Figure 1: UT TRACE Model

The geometry of the fuel element and surrounding flow area (Figs. 2 and 3) is modeled as a hexagon with an inner radius (i.e., the largest circle centered in and bounded by the hexagon) ½ of the pitch. A large fraction of the model is occupied by the fuel element, leaving a relatively small flow area. End fittings have more complex geometry and are approximated using hydrodynamic characteristics. Equations 1-4 (following) provide data required in the TRACE input file.

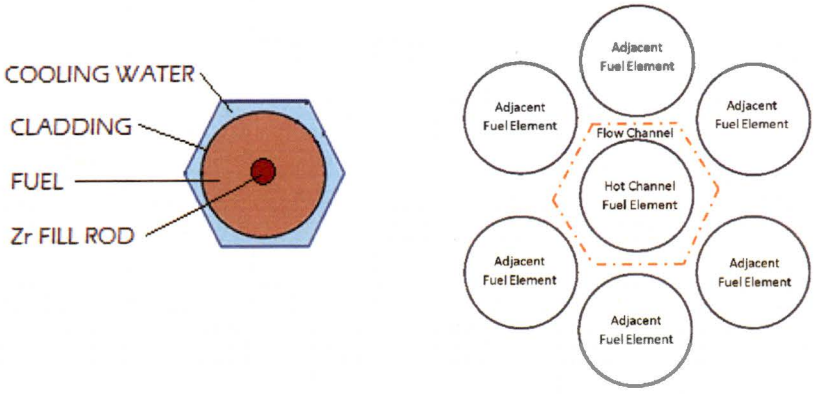

Figure 2: Flow Channel for UT TRIGA

The area of the flow channel (A) is the area of the hexagon less the area of a fuel element. Using p_e as pitch and D_F as the diameter of the fuel element, the area of the flow channel is given by:

$$A = \frac{\sqrt{3}}{2} \cdot p_e^2 - \pi \cdot \left(\frac{D_F}{2}\right)^2 \qquad \text{Eqn 1}$$

The wetted perimeter (P_w) is the perimeter of the fuel element:

$$P_W = \pi \cdot D_F \qquad \text{Eqn 2}$$

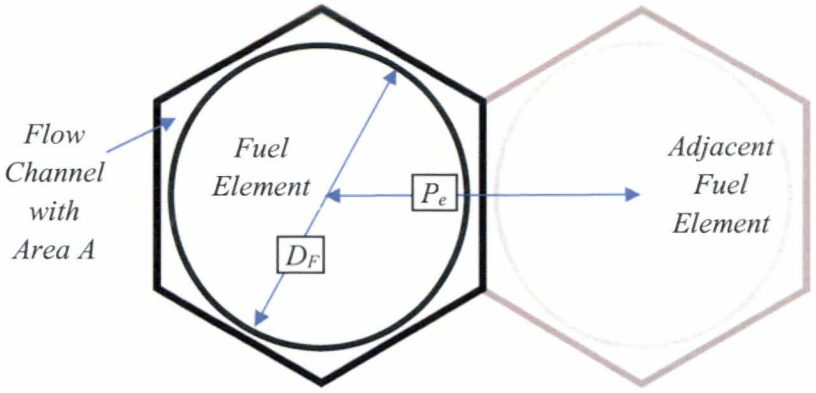

Figure 3: Pitch and Fuel Element Diameter And Relation to Flow Channel

Non-circular pipes are approximated from the flow area and the wetted perimeter (P_W) with an equivalent hydraulic diameter (D_h) calculated using:

$$D_h = \frac{4 \cdot A}{P_W} \qquad \text{Eqn 3}$$

Substituting equations 1 and 2 into equation 3 yields the following expression for the hydraulic diameter:

$$D_h = \frac{4}{\pi \cdot D_F} \cdot \left[\frac{\sqrt{3}}{2} \cdot p_e^2 - \pi \cdot \left(\frac{D_F}{2} \right)^2 \right] = \frac{2 \cdot \sqrt{3}}{\pi} \cdot \frac{p_e^2}{D_F} - D_F = D_F \cdot \left[\frac{\sqrt{3}}{2} \cdot \frac{p_e^2}{D_F^2} - 1 \right] \qquad \text{Eqn 4}$$

2.2 Thermal Hydraulic Loss Factors

Pressure drops (head loss) across hydraulic components are the product of the fluid flow and factors such as the coefficient of friction between the fluid and the pipe wall, changes in flow area and diameter, flow channel surface roughness, and/or flow channel length. Standard practice defines the characteristics that determine head loss as coefficients, or K factors based on experimentally derived correlations to support conservation of energy and momentum calculations for fluid flow. The surface roughness for TRIGA fuel elements is 6.998E-6 ft.[7] Correlation of K factors with geometry and flow are based on historical, experimental measurements with cylindrical pipes. The correlations are extended to rectangular ducts; non-circular cross sections are reduced to a flow area and hydraulic diameter developed by assuming the area is a circular geometry. These correlations apply after flow is fully developed following geometry perturbations that create turbulence. The geometry inherent in TRIGA fuel challenges application of standard formula to calculate the K factors:

- The fuel element end fittings are partially inserted in grid plate penetrations that fix the position of the fuel elements in the core, causing abrupt flow area expansion and contraction at upper and lower grid plates that affects end fitting flow conditions.

- Flow entrance to and exit from the flow channel between the grid plates is directed by fins, a center

[7] Oregon State University, Model Editor File for the OSTR thermal hydraulic Model (private communication)

pin, and a conical shape (with part of the structure extending into the volume bounded by grid plate penetrations); the wetted perimeters vary continuously from entrance to exit for each end fitting.

- The interface between adjacent fuel channels is not separated by a physical boundary, and differential pressure between adjacent flow channels can support cross-channel flow, although analysis has shown that any cross-flow is small and has "no effect on fuel temperature" with a slight increase in critical heat flux ratio[8]; cross flow is neglected in this analysis.

Therefore, thermal hydraulic analysis to support relicensing was developed to independently model thermal hydraulic performance at the end fittings from (1) first principles, (2) the TRACE thermal hydraulics code, and (3) the FLUENT computational fluid dynamics code. The results of experiments in the TRIGA core were used to evaluate UT TRIGA-specific K factors based on actual fuel element geometry. The values determined from the UT research program (Table 1) were used in modeling for TRACE calculations.

Table 1: UT TRIGA Specific K Factors

APPLICATION	K Factor
TRIGA Lower Channel	1.63
TRIGA Upper Channel	1.12

2.3 Hydrostatic Pressure

Cooling media pressure and temperature specifications associated with break components are based on local environmental conditions (barometric pressure, confinement pressure regulation) and the pool water (level and temperature). The NETL building is approximately 240 m above sea level, and the reactor bay confinement system is designed to control differential pressure to 0.06 in. below atmospheric pressure (minimal compared to atmospheric pressure). Total pressure at the top of the core is:

$$p_T = 96\{KPa\} + p_{H_2O} \qquad \text{Eqn 5}$$

Pool water is nominally 7.25 m above the core, with a minimum of 5.25 m. Pool water temperature is nominally 25-27 °C, and administratively limited to less than 49 °C. Where g denotes the gravitational constant (9.8 $m \cdot s^{-2}$), the pressure (p_{H2O}) exerted by a column of water (at density ρ in $kg \cdot m^{-2}$and height h in m) is given by:

$$p_{H_2O} = \rho \cdot g \cdot h \qquad \text{Eqn 6}$$

Breaks using the same parameters are connected to the entrance of the downcomer and exit from the flow channel (representing the exit of the core). Pressure boundary conditions for the limiting cases are provided in Table 2, converted to British units for TRACE input.

Table 2: LCC Temperature & Pressure

Condition	Temp (°F)	Pressure (Psia)
Limiting	120.2	21.3
Nominal	77	24.2

[8] Armed Forces Radiobiology Research Institute (AFRRI) submittal of Safety Analysis Chapters 4 and 13 to the USNRC (ML101650422, submitted on March 4, 2010)

2.4 Heat Structure Modeling

The heated length of the fuel element is modeled as a TRACE heat structure. The heat structure simulates the zirconium fill rod at the center of the fuel element, the fuel matrix, the gap between the fuel and cladding, and the cladding. The UT TRIGA heat structure is segmented by 15 radial and 15 axial coordinates into cells that transmit heat from the fuel element to the cooling channel. The UT TRIGA model uses a gas gap heat transfer coefficient[9] of 500 Btu $h^{-1} ft^{-2} °F^{-1}$, (2840 W $m^{-2} K^{-1}$). The flow channel includes non-heated lengths that are not part of the heat structure above and below the heated length representing integral graphite reflector and end fittings (with a space in the upper end fitting for fission gas collection incorporated above the upper graphite reflector).

2.5 Power/Reactivity Application

Fuel element power was used as an input for steady-state and LOCA analysis, supporting cases with time-dependent reactivity variation, and as an input to extend average fuel element power analysis to the hot channel. Reactivity was used as an input for transient analysis, supporting pulsing, control rod withdrawal, and LOCA analyses. Reactivity transients were used to generate time dependent power levels for a fuel element representing the core average in pulsing and control rod withdrawal analysis. The time dependent average element power level was scaled by the core peaking factor to represent the hot channel time dependent power calculations. For LOCA analysis, the time dependent behavior of power following shutdown was evaluated and developed using reactor kinetics for fission power and the method of ANSI/ANS-5.1-2014 (equations 7 and 8) for decay heat from fission products. For an irradiation interval of time T, a decay time of t, and irradiation intervals i and a constant fission rate of unity, decay heat power (F, units of MeV/fission) can be represented analytically as a function using analytic fit constants α and β (the fit constants are provided for all 23 components in the standard):

$$F_i(t, T_a) = \sum_{j=1}^{23} \frac{\alpha_{i,j}}{\lambda_{i,j}} \cdot exp(-\lambda_{i,j} \cdot t) \cdot [1 - \exp(-\lambda_{i,j} \cdot T)] \qquad \text{Eqn 7}$$

Assuming a single power generation interval and a long operating time, this reduces to:

$$F(t) = \sum_{j=1}^{23} \frac{\alpha_j}{\lambda_j} \cdot exp(-\lambda_j \cdot t) \qquad \text{Eqn 8}$$

The ratio of decay heat power to initial reactor power depends on a reactor specific energy generation per fission (MeV/fission) that is also used in TRACE transient calculations. The MCNP burnup analysis output tabulates fission energy yield data (Q value) as given in Table 3.

Table 3: Fission Energy Yield from MCNP Analysis

Nuclide	Q-Value (MeV)
92235	180.88
92238	181.31
94239	189.44
94241	188.99

[9] The University of Texas Safety Analysis Report, Revision 1.01 (5/91)

The fraction of energy produced by each fissionable material (Table 4) used in TRACE analysis is taken from an MCNP burnup calculation supporting the neutronics report. Estimates of the fraction of isotope 92235 fissions at greater than thermal energy is assumed to have Q values consistent with isotope 92238.

Table 4: Fission Isotope Nuclear Characteristics[10]

Nuclide	Fraction	Fission Cross-section (b)	Energy Range	Fissions at Energy
92235	19.8%	585.1	<0.625 eV	94.28%
		274.4	0.625 ev – 100 kev	4.99%
92238	80.2%	1.241		
		0.03064	>100 kev	0.72%

The kinetics treatment used fission product nuclear characteristics (precursor fractions, decay constants, and the generation time) from MCNP adjoint calculations given in Table 5. Thermal/non-thermal fission fractions are taken from the MCNP burnup calculations.

Table 5: Delayed Neutron Precursor Group Characteristics

	β_i	Standard Deviation	Energy (MeV)	Standard Deviation	λ_i (s^{-1})	Standard Deviation	$T_{1/2}$ (s)	Standard Deviation
1	0.00022	0.00005	0.40605	0.00460	0.01334	0.00000	51.960	0.004
2	0.00138	0.00013	0.47218	0.00202	0.03273	0.00000	21.178	0.001
3	0.00138	0.00012	0.44217	0.00202	0.12080	0.00000	5.73797	0.00005
4	0.00296	0.00019	0.55867	0.00181	0.30295	0.00001	2.28799	0.00008
5	0.00113	0.00011	0.51895	0.00294	0.85032	0.00004	0.81516	0.00004
6	0.00059	0.00009	0.53926	0.00495	2.85537	0.00021	0.24227	0.00002

Heat generation distribution in the heat structure is based on mesh tally calculations from MCNP modeling described in the neutronics report. The MCNP mesh tally provides average fission density at 225 locations throughout the fuel rod. These 225 locations consist of equal volume segments of the fuel with 15 radial segments and 15 axial segments. The normalized mesh values were applied to locations in TRACE. . This 15x15 matrix was used as a power distribution profile in TRACE. Equal volume segments allow direct averaging of temperatures in the fuel

MCNP adjoint calculations were used to generate estimates of the prompt neutron generation time and effective delayed neutron fractions. The MCNP calculations produced an estimated prompt-neutron generation time of 43.81±0.53 μs (Table 6). The 1992 Safety Analysis Report for the UT TRIGA cited a prompt generation time of 41 μs, which is reasonably consistent with that calculated by MCNP; the MCNP calculated value utilizing current parameters is used in this report.

The effective delayed neutron fraction has historically been used as 0.007 for the UT TRIGA. The MCNP calculated value for β_{eff} was 0.00737±0.00006 (Table 6). Calculating pulsing reactivity in units of $ based on β_{eff} of 0.007 represents 91% of the nominal pulsed reactivity. Data from two series of reactor pulses with varying reactivities were analyzed using the Fuchs-Hansen pulse model modified to evaluate β_{eff} from the convergence of iterative calculations. Pulses from November 2018 were found to have a β_{eff} of 0.007306, and from March 2020 to have a β_{eff} of 0.007382.

[10] https://wwwndc.jaea.go.jp, Fission at Energy from MCNP burnup calculation

Table 6: MCNP Calculated Reactivity Parameters

Parameter	Estimate	Standard Deviation
Generation Time	43.81 μs	0.53 μs
β_{eff}	0.00737	0.00006

2.6 User Defined Materials

Zirconium properties are provided in Table 7. The zirconium fill rod is slightly smaller than the center hole of the fuel element. Therefore, the standard zirconium density was reduced by the ratio of the zirconium rod volume to the whole center-hole volume.

Table 7: Zirconium Properties

Temperature °F	Density lbm/ft^3	Heat Capacity (C_p) Btu/lbm-°F	Thermal Conductivity Btu/h-ft-°F	Emissivity
-99.4	328.18	0.082284	14.562	0.8
260.6	328.18	0.102199	12.4812	0.8
620.6	328.18	0.122114	11.9592	0.8
980.6	328.18	0.142029	12.4812	0.8
1340.6	328.18	0.161943	13.6944	0.8
1700.6	328.18	0.181858	15.0228	0.8
2240.6	328.18	0.211731	16.6392	0.8
4481.2	328.18	0.335679	21.6392	0.8

Reference values[11] for specific heat capacity (C_p) and thermal conductivity (k_c)of TRIGA fuel are:

- $C_p = 0.018 \pm 0.009$ watts [$cm^{-1}\,°C^{-1}$]
- $k_c = 2.04 + 0.00417 \times T$ [$W\,s^{-1}\,cm^{-3}\,°C^{-1}$] (note that this is given as a function of material temperature T)

These formulae were converted to British units and used to generate tabular values (Table 8) for TRACE.

Table 8: Uranium-Zirconium Hydride (Fuel)

Temperature °F	Density lbm/ft3	Heat Capacity (Cp) Btu/lbm-°F	Thermal Conductivity Btu/h-ft-°F	Emissivity
-65.6	374.5	0.029754	10.16021	0.8
294.4	374.5	0.091403	10.16021	0.8
654.4	374.5	0.153051	10.16021	0.8
1014.4	374.5	0.2147	10.16021	0.8
1374.4	374.5	0.276349	10.16021	0.8
1734.4	374.5	0.337997	10.16021	0.8
2274.4	374.5	0.43047	10.16021	0.8
4548.8	374.5	0.814165	10.16021	0.8

[11] E-117-833, The U-Zr_x Alloy: Its Properties and Use in TRIGA Fuel (Simnad, General Atomics Project No. 4314)

2.7 Temperature Feedback

Temperature feedback is incorporated in the reactivity transient analysis to support pulsing and control rod withdrawal event analyses. General Atomics[12] indicates that the fuel temperature coefficient (water reflected) is convex, with a minimum occurring about 300°C. An analysis at AFRRI[13] based on DIF3D (Argonne National Laboratory, diffusion and transport theory code) calculations show convex fuel temperature reactivity structure from 10-1000°C for TRIGA fuel. Standard MCNP cross sections are available in intervals of about 300°C; it is not possible to get data from calculations where cross-sections are separated by 300°C that would provide accurate data for derivation of reactivity coefficients over the range of operation. Therefore, an auxiliary code distributed with MCNP (MAKXSF) was used to generate data over the range of interest. Although fuel temperature and water temperature coefficients are generally considered independently, they are coupled. The temperatures used for generating these cross sections are shown in Table 9.

Table 9: Cross Section Temperatures (°F)

Fuel	98.33	118.13	344.93	458.33	571.73	841.73	1111.73	1291.73	1471.73	1651.73
Water	76.73	76.73	80.33	107.33	134.33	168.53	188.33	215.33		

Criticality calculations with the MCNP model of neutronics analysis were performed using all permutations of temperatures indicated. Fuel temperature, water temperature, and the associated excess reactivity for each calculation was used to generate a reactivity function of the two temperatures. The function was used to evaluate values ½ degree above and ½ degree below specific fuel temperatures with water temperature held constant, and then varying water temperature with constant fuel temperatures. The results are provided graphically at selected fuel temperatures, fuel temperature reactivity coefficients for a series of constant moderator temperatures (Fig. 4) and moderator temperature coefficients for a series of constant fuel temperatures (Fig. 5).

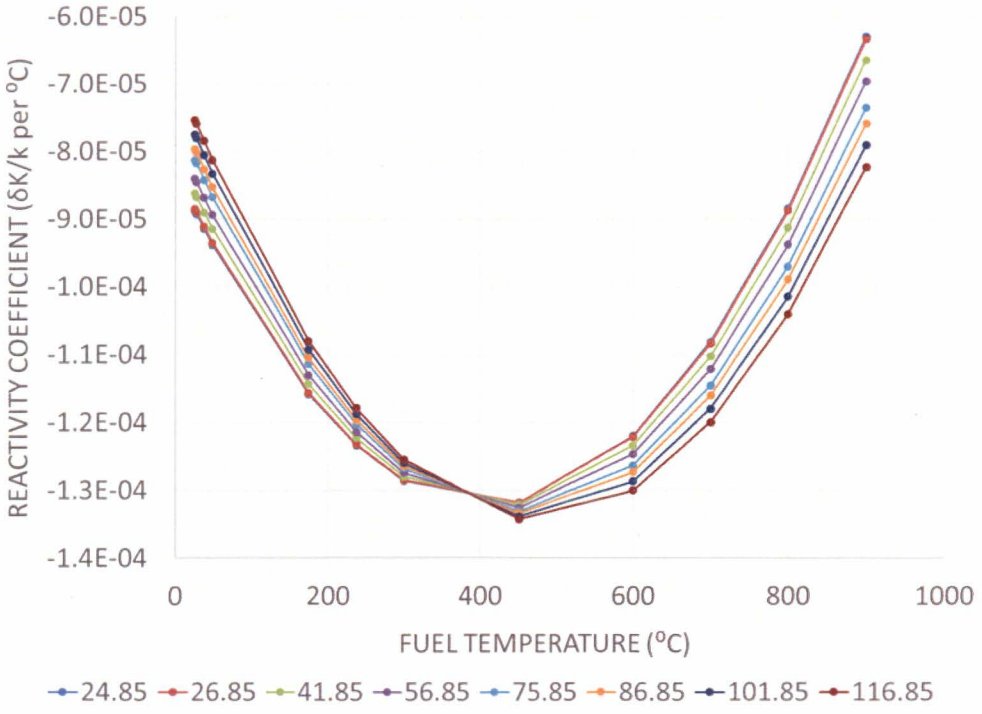

Figure 4: Temperature Coefficient of Reactivity for the Fuel Versus Fuel Temperature (shown at a variety of fixed coolant temperatures)

[12] Simnad op. cit.
[13] AFRRI op. cit.

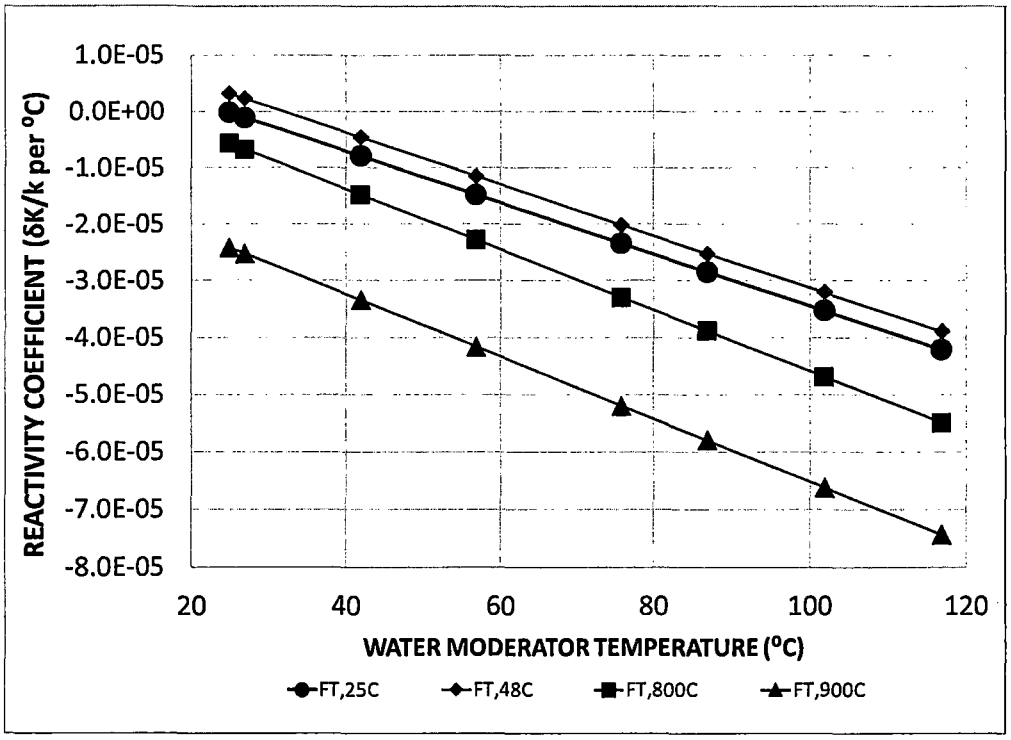

Figure 5: Water Temperature Coefficient of Reactivity Versus Water Moderator Temperature (shown at a variety of fixed fuel temperatures)

The maximum variation in the fuel temperature reactivity coefficient at low temperature (with respect to water temperature) is on the order of 10% from nominal water temperature to temperatures near boiling in the core. The water temperature change is dominated by the decrease in water density as temperature increases; lower water density increases scattering length and reduces moderation in the cooling channels. As fuel temperature increases there is less absorption in the fuel matrix and consequently more neutron scattering out of the fuel matrix into the water. These competing effects cause the difference with respect to water temperature to converge and then reverse the difference at higher fuel temperatures. At constant fuel temperature, the moderator temperature coefficient change is almost linear with respect to moderator temperature change from ambient temperature values to near boiling at the core hydrostatic pressure.

The calculations based on DIF3D[14] suggest fuel coefficient reactivity ranges from -8×10^{-5} to -1.2×10^{-4} $\Delta k/k\ °C^{-1}$ for a TRIGA core with a circular grid plate (the UT TRIGA has hexagonal pitch), or -4.5×10^{-5} and -6.8×10^{-5} $\Delta k/k\ °F^{-1}$. This is in reasonable agreement with this analysis. The temperature coefficient data is used in TRACE to determine temperature reactivity coefficient feedback for transient analysis.

3.0 VALIDATION

The neutronics report identifies instrumented fuel elements (IFEs) in the current core (1.1 MW core, 113 elements) in positions B03 and B06 generating 15.82 kW and 15.39 kW respectively. The UT TRIGA administratively limits power operation to 950 kW, 86.4% of the licensed power level; therefore, the power levels generated in the thermocouple elements at nominal full power operations are 13.66 kW and 13.29 kW. Normal operations occur with a pool (cooling water) temperature of 25°C (77°F). Pool level during normal operations is 7.25 m (23.8 ft) above the core; therefore, hydrostatic pressure is 24.2 psia for normal operations. A series of calculations with nominal conditions was performed to allow comparison of observed power levels and temperatures to those generated by TRACE model simulating nominal operations.

[14] AFRRI

3.1 Steady State

Each IFE has three thermocouples embed in the fuel matrix, with the thermocouple exhibiting the highest temperature connected to the fuel temperature measuring channels. The temperatures of the thermocouple locations used in the measuring channel were calculated using the TRACE model. One thermocouple was replaced in February 2016 and indicated high temperature indication from installation to the present. This is typical behavior for replacing a partially depleted IFE with one containing fresh fuel: the amount of ^{235}U is higher in the replacement element, there are no fission product poisons, and the fuel tolerance that allows insertion into the cladding impedes heat transfer (fuel swelling during operation eventually closes the gap). These transient conditions have a significant effect on power distribution and heat transfer.

However, the material composition for the IFE in the neutronics analysis was based on average isotopic values at initial fuel loading, which included fission products and transuranic isotopes (all standard fuel in initial loading had prior power history). To avoid associated complications, the baseline data for validation is taken from December 2015 through February 2016 covering IFE load configurations in Table 10. Temperature calculations are extremely sensitive to power generation, so a correction was made for MCNP material composition with the fresh IFE to more accurately reflect actual fuel loading with no fission products or transuranics in the MCNP material. Power distribution was developed from calculation of fissions in each element using the MCNP model as modified.

Table 10: IFE CONFIGURATIONS AND INSTRUMENT INDICATIONS

DATE	POWER	IFE	FT1	IFE	FT2
12/18/15	0.92	10878 (B03)	325°C	10708 (B06)	364°C
01/16/16		*IFE 10708 replaced with IFE 10809*			
01/27/16	0.92	10878 (B03)	325°C	10809 (B06)	427°C
02/01/16	0.93	10878 (B03)	319°C	10809 (B06)	420°C
02/01/16		*FT1 and FT leads exchanged*			
2/2/2016	0.94	10809 (B06)	419°C	10878 (B03)	322°C

Power distribution data from the neutronics analysis is assumed to apply prior to the instrumented fuel element replacement and scaled to 92% consistent with the power level when the temperature data was taken. TRACE calculations indicate temperature 10°C below the measuring channel that used IFE 10708 and 36°C above the channel with IFE 10848 before element 10708 was removed After 10708 was removed and 10809 installed, the TRACE calculations show temperature 26°C elevated over 10848 and 21°C below 10809.

Table 11: TRACE AND INSTRUMENT COMPARISON

INITIAL CONFIGURATION			
ELEMENT	POWER	TRACE/MCNP	FT
10708	13.61	354°C	364°C
10848	13.24	345°C	319°C
FOLLOWING IFE EXCHANGE			
ELEMENT	POWER	TRACE/MCNP	FT
10809	15.30	394°C	420°C
10848	13.30	346°C	325°C

Comparison of the TRACE calculation and observed data shows reasonably close agreement (within ±8.5% of the measured value), with differences principally attributed to the IFE material composition in the MCNP model used to calculate the power generation rate.

3.2 Pulsing Operations

The TRACE calculations were compared to historical data to validate the accuracy of the method used. Historical pulse data (reactivity addition, peak pulse power, and maximum temperature from the fuel temperature measuring channels) was compiled, with incomplete data purged. There is significant scatter in power level (Fig. 6) and temperature (Fig. 7) data with some outliers but, the results overall show good agreement AND provide a basis for validation. Pulse records do not include factors with potential to affect pulse characteristics such as initial fuel temperature, pool temperature, or recent operating history that might explain some of the scatter in the data. Since TRACE calculations are for individual elements, peak pulse power level was distributed across the core for comparison to historical data. Although there is significant scatter and outliers in historical pulse power level data, it is clear that qualitatively the TRACE data agrees well with historical data.

A comparison of peak temperature to historical pulsing data required adjusting the average pulse power to the power generated in the IFE by the ratio of the power in the instrumented fuel elements (identified in the neutronics report) to the average element power. The fuel matrix in IFEs is fabricated with milled channels to accommodate thermocouple leads, and the thermocouples are installed in fuel penetrations extending from the outer surface to near the inner surface of the fuel. Consequently, the volume of the fuel in the IFE is a few percent lower than a standard fuel element. One IFE was installed in 2016 while the MCNP model did not account for higher loading of fresh fuel. All fuel material specifications in the MCNP model used to calculate power generated in the IFE assumed the same density as standard fuel elements, while initial loading varied. Even with the complications created by MCNP modeling, data scatter, and outliers the TRACE calculations agree well with observed data.

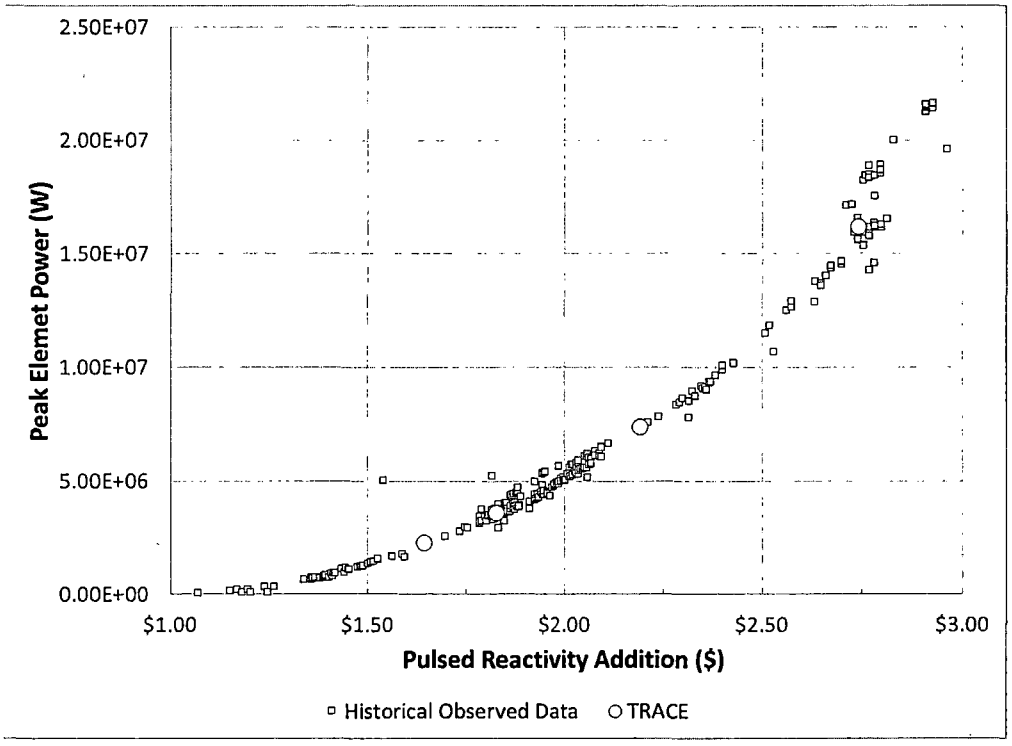

Figure 6: Peak Element Power Level Versus Pulse Reactivity Addition from UT TRACE Calculation Compared to Observed Historical Data

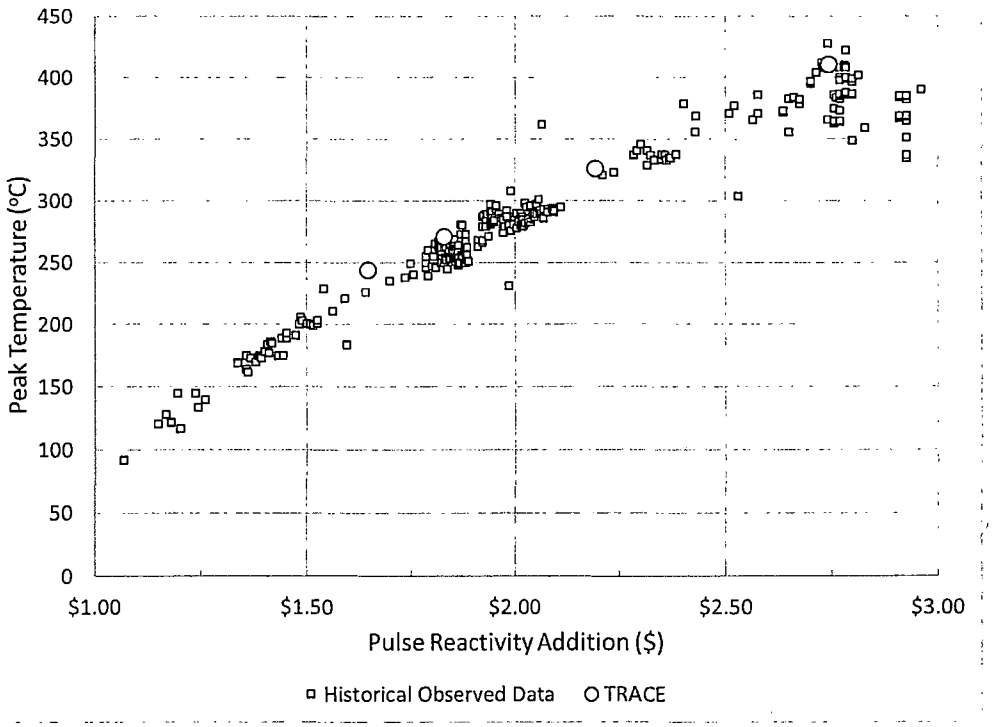

Figure 7: Peak Fuel Temperature Versus Pulse Reactivity Addition from UT TRACE Calculation Compared to Historical Data

3.3 Conclusion

Fuel temperatures indicated by the fuel temperature measuring channels, and power and temperature from historical records of pulsing, were compared to data generated with TRACE calculations. The comparison demonstrates that the TRACE model predicts thermal hydraulic performance of the UT TRIGA reactor with reasonable accuracy.

4.0 LIMITING CORE CONFIGURATION

4.1 Steady-State Power Level

The neutronic analysis indicates that for a licensed power of 1.1 MW, the maximum power in any element is 22.14 kW with 84 elements. With a maximum potential instrument error of 10%, the maximum power in the hot channel could be as high as 24.34 kW. This UT TRIGA hot channel power level is well within TRIGA operating experience, less than reported values for the AFFRI TRIGA reactor (35.3 kW) and the TRIGA conversion reactor at the University of Wisconsin (26.04 kW)[15], and less than the 30 kW value cited in ANL RERTR TM 07 01 (which references the MNCR reactor at 33.2 kW).

To evaluate steady-state performance of the LCC, a series of TRACE calculations were performed for the UT TRIGA for fuel element power levels between 5 kW and 60 kW under limiting core conditions. Temperature dependence of the fuel versus power is shown in Fig. 8 for the hot channel, while the radial and axial temperature distribution across the hot channel are shown in Figs. 9 and 10. Fuel element power at 44.9 kW is found to result in a maximum fuel temperature during steady state operations of 1149.9°C, essentially

[15] University of Wisconsin LEU Conversion Report (Request for Amendment No. 17 to Facility License No. R-17, 08/25/2008)

the maximum safety limit if cladding temperate is greater than 500°C. Fuel element power at 36.6 kW results in 948.1°C, approaching the 950°C safety limit if cladding temperature is less than 500°C.

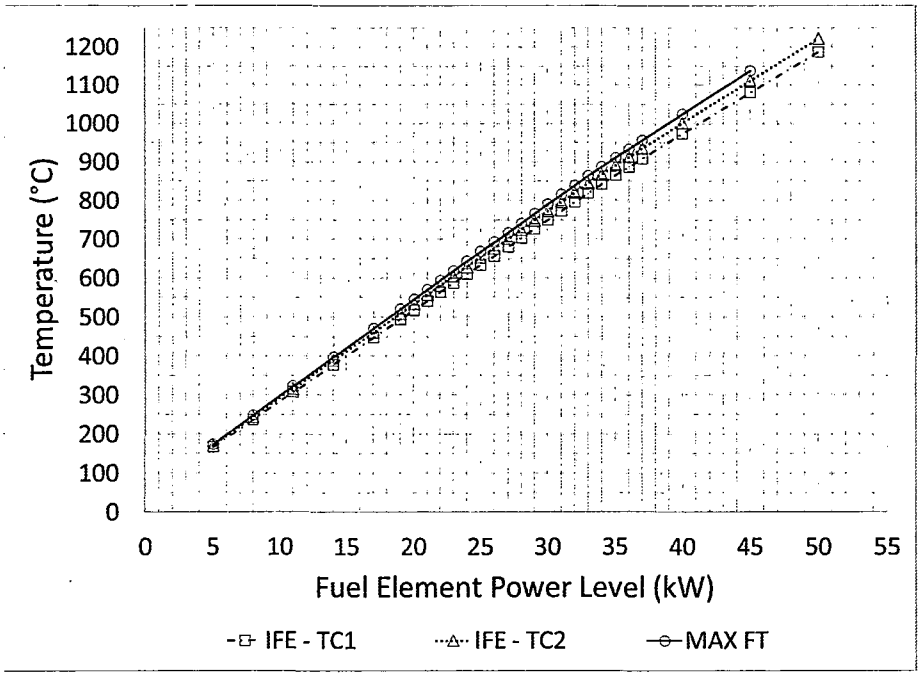

Figure 8: LCC Steady-State Fuel Temperature Versus Fuel Element Power at Each Thermocouple and at the Maximum Fuel Temperature Location

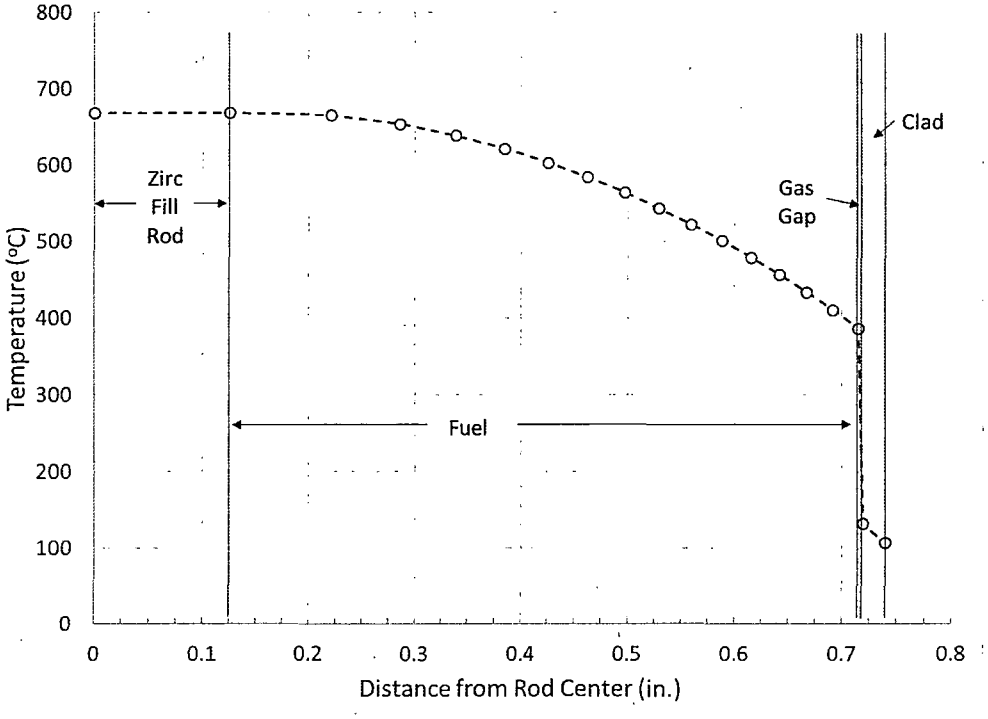

Figure 9: LCC Hot Channel Radial Fuel Temperature Profile at Hottest Axial Position

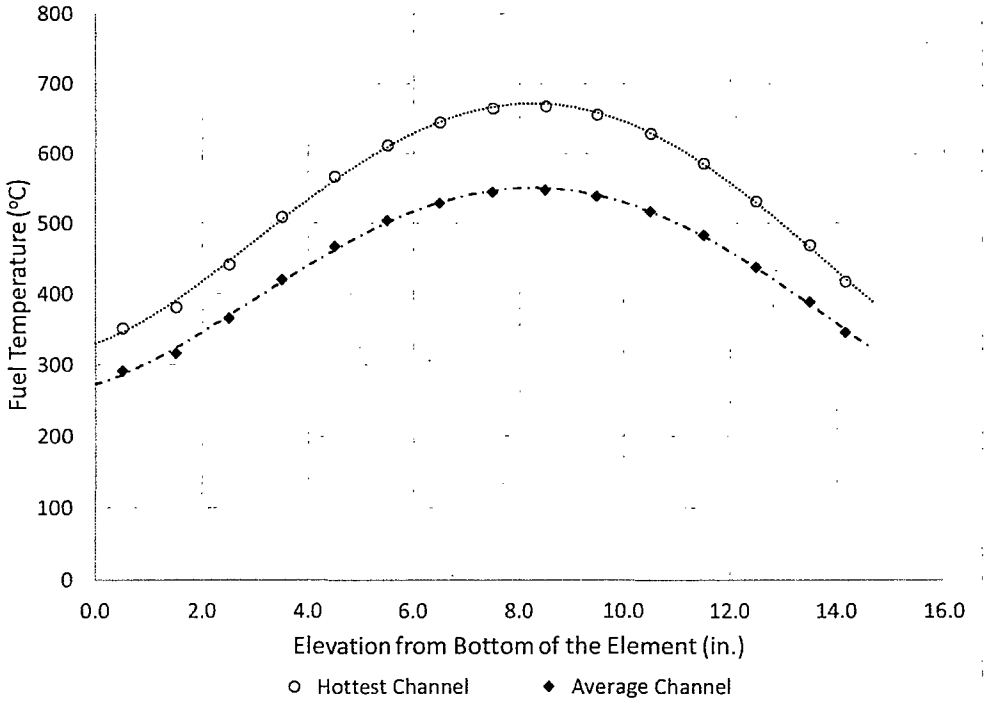

Figure 10: LCC Hot Channel Axial Radial Fuel Temperature Profile

The critical heat flux that leads to burnout is calculated by the Bernath correlation (with variables defined in Table 11):

$$CHF_{BO} = \left[10890 \cdot \frac{D_e}{D_e + D_i} + V \cdot \frac{48}{D_e^{0.6}}\right] \cdot \left(\left[57 \cdot \ln P - 54 \cdot \frac{P}{P + 15} - \frac{V}{4}\right] - T_B\right) F(t_a) \qquad \text{Eqn 9}$$

Table 11: Bernath Correlation Variables

D_e	Hydraulic diameter	ft	Previous formula
D_i	Heater surface diameter	ft	Fuel element diameter
V	Pressure	Psia	Calculated by TRACE
P	Velocity	$ft \cdot s^{-1}$	Calculated by TRACE
T_B	Coolant Temperature	°C	Calculated by TRACE

A series of calculations were performed using the Bernath correlation to determine the relationship between element power and the minimum CHFR along a rod in limiting core conditions (Fig. 11). The limiting value of 2.0 for CHFR occurs at 56 kW generated in the hot channel, in agreement with analysis cited in ANL RERTR TM 07 01. With the UT TRIGA hot channel operating at 24.35, the critical heat flux ratio is 4.69.

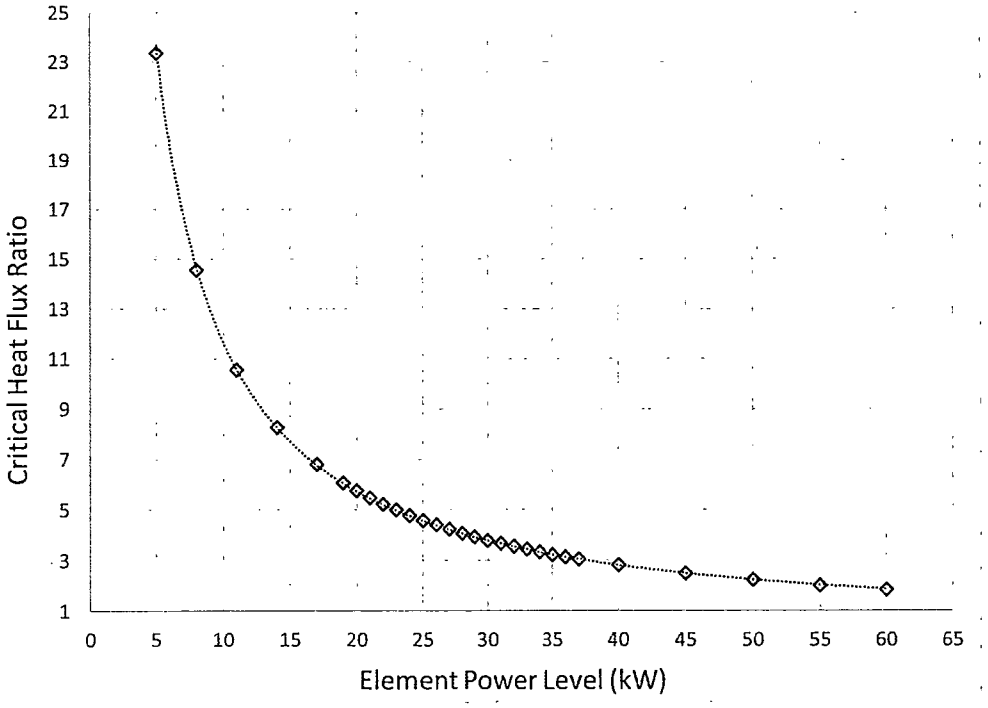

Figure 11: CHFR (Bernath Correlation) Versus Fuel Element Power

The critical heat flux ratio varies along the length of the hot channel fuel element at full power as indicated in Fig 12. The minimum CHFR is slightly above the center of the section of the fuel element that contains fuel.

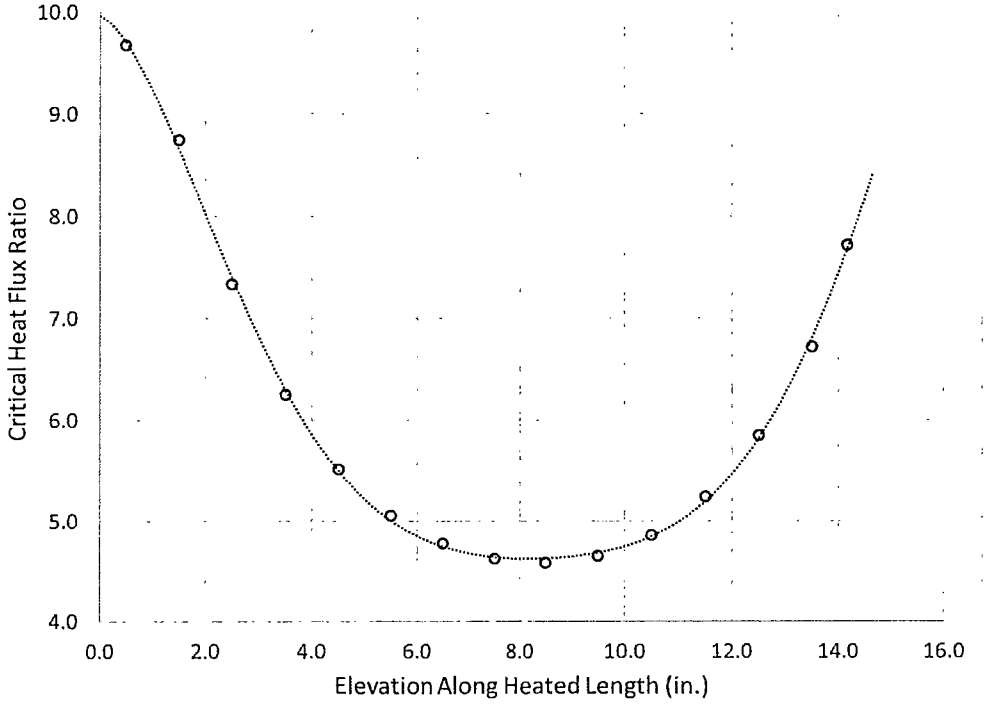

Figure 12: CHFR Hot Channel Axial Values from the Bernath Correlation for UT TRIGA Fuel Element Operating at 24.34 kW

With the hot channel operating at 24.34 kW, the maximum temperature in the core is calculated by TRACE at 650°C, approximately 300°C below the 950°C safety limit. The hot channel power is 12.3 kW below the 36.6 kW that would approach the fuel temperature safety limit. The hot channel element CHFR with power level of 24.34 kW is 4.69 - significantly above the CHFR limit of 2.0. The LCC hot channel is 33.7 kW below 55 kW, the power level that would result in a CHFR of 2.0. Based on these results the LCC characteristics are well within the safety margins.

4.2 Pulsing Operations

Pulsing reactivity calculations were performed in TRACE for the LCC hot channel using $3, $4, $5, $6, and $7 insertions with initial conditions approximating shutdown power levels. The calculations were performed in two steps: (1) reactivity addition was used to calculate time-dependent core power level of an average fuel element and (2) the time/power profile was used in second step, with the power of the second step scaled by the hot channel peaking factor to represent the LCC hot channel fuel element. The peak power as a function of pulsed reactivity is shown in Fig. 13, and the time-development of the power pulse for the reactivity insertions in Fig. 14. The $7 insertion is not included so that the remaining data can be shown on a reasonable scale.

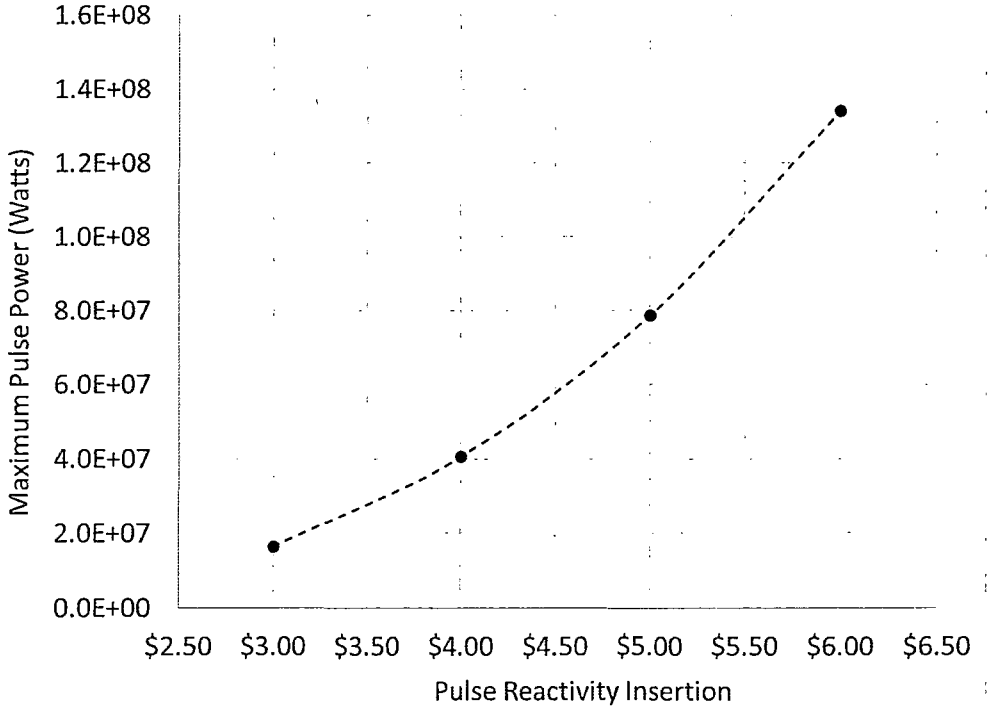

Figure 13: Hot Channel LCC Peak Power Level Versus Reactivity Insertion

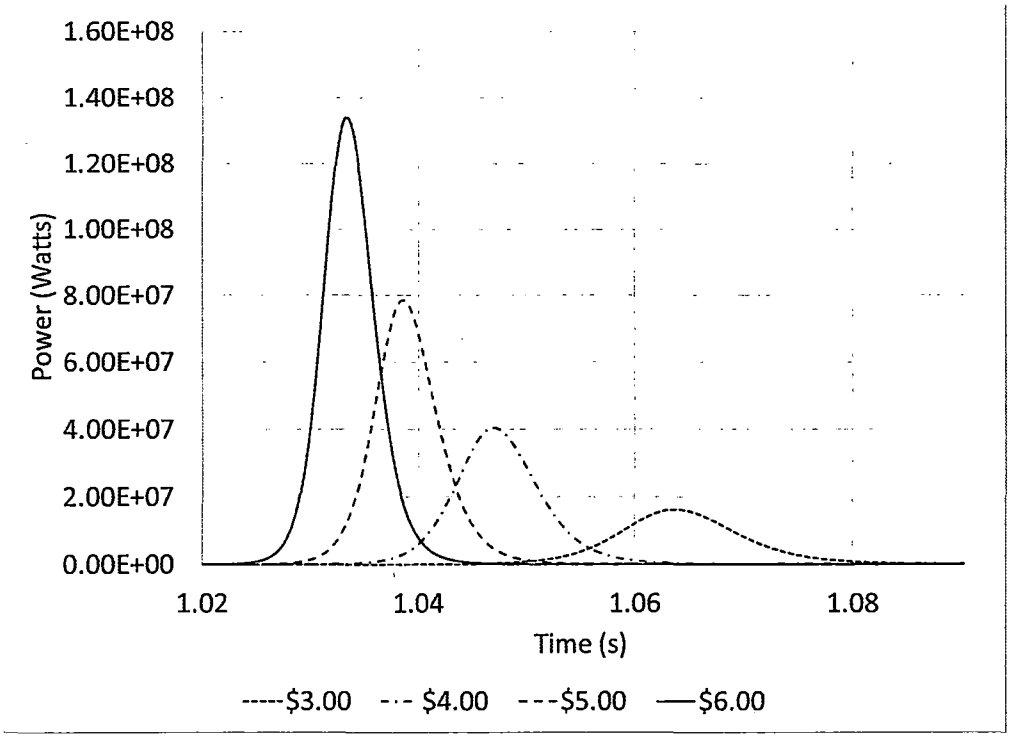

Figure 14: LCC Pulse Power Versus Time for Varying Reactivity Insertions

A $3 insertion resulted in a peak temperature of 378°C. As shown in Fig. 15, the temperature limit was not exceeded for any reactivity insertions below $6 (with a 130°C or 16% margin at $6). The temperature safety limit was not also exceeded at a $7 reactivity insertion. Time dependent behavior is shown in Fig. 16.

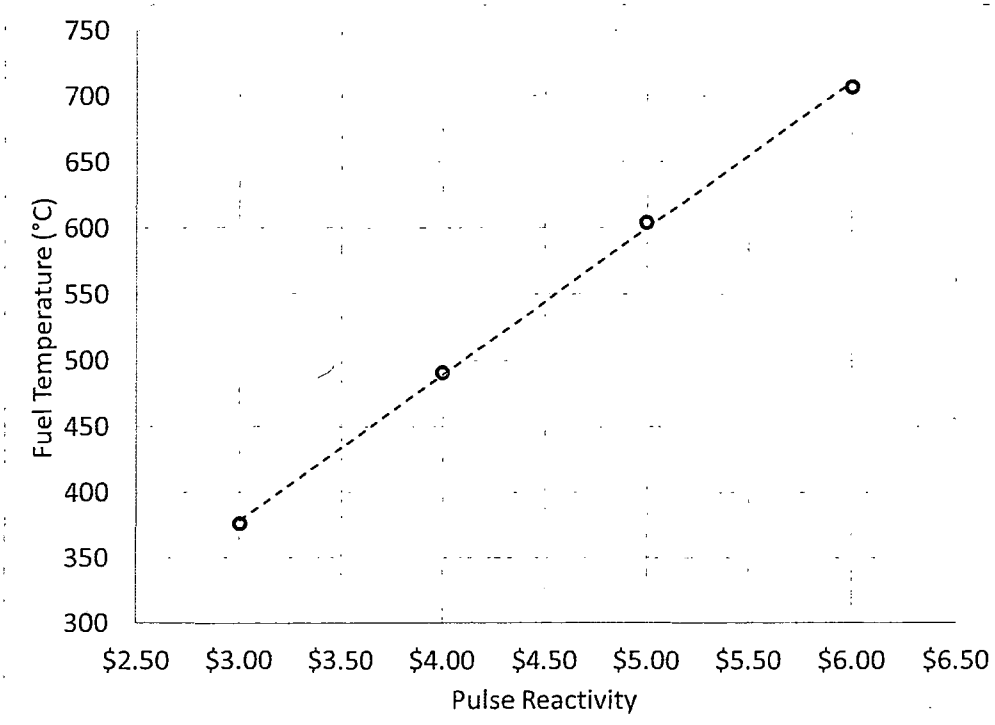

Figure 15: LCC Hot Channel Peak Fuel Temperature Versus Pulse Reactivity Addition

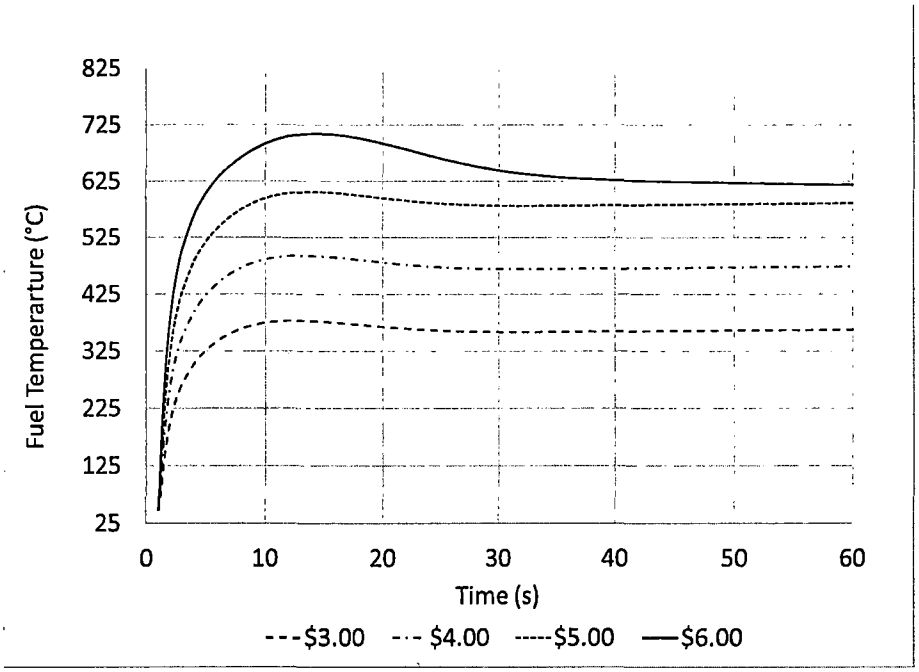

Figure 16: LCC Hot Channel Fuel Temperature Versus Time from Pulse Initiation for Several Pulse Reactivity Additions

The maximum effect of pulsing at power was evaluated. The average channel was characterized with (1) simulated incremental insertion to $4, (2) a period at $4 to establish initial conditions, and (3) total reactivity addition of $7. The resulting time dependent power was taken from the calculation, scaled by the hot channel peaking factor to simulate the hot channel, and used in a time dependent power calculation. The maximum fuel temperature in the hot channel prior to the pulse was 252 °C at 8.25 kW (corresponding to a core power of 43.3 kW). Following the pulsed insertion of $3, the peak hot channel fuel temperature was 579°C and peak power 74.4 kW (Fig. 17).

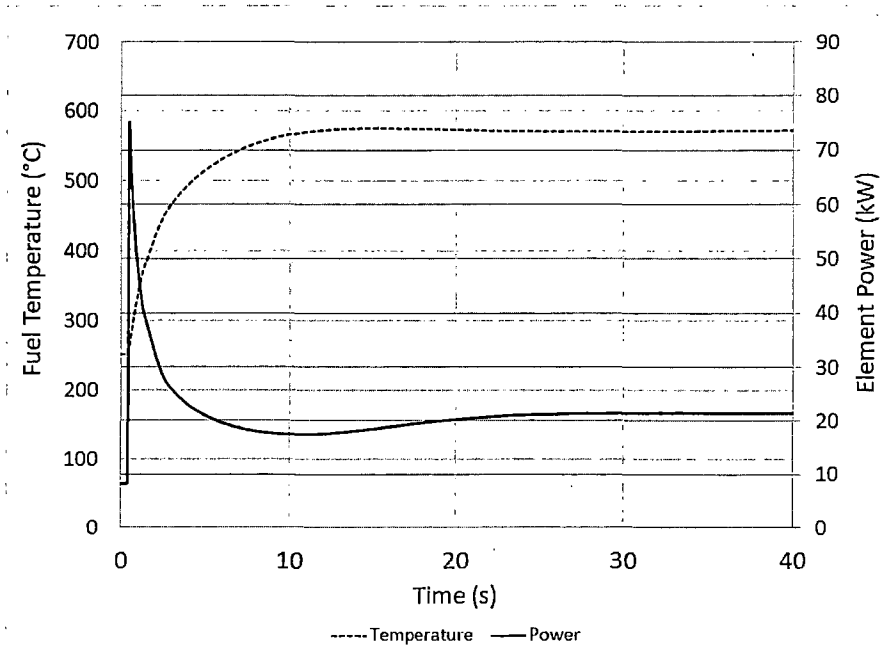

Figure 17: LCC Hot Channel Fuel Temperature and Element Power Versus Time for a $3 Pulse from Steady-State Operation with Element at an Initial Power of 8.25 kW and Fuel Temperature of 252 °C (Note that pulse was initiated at 0.5 seconds on the time scale shown)

A maximum pulsed reactivity addition of $3.00 from low power is adequate to maintain fuel element temperature less than 50% of the limit. Maximum pulsed reactivity addition with the reactor operating at the balance of excess reactivity will not exceed the limiting fuel temperature at any initial achievable power level.

4.3 Continuous Reactivity Addition Transient (Control Rod Withdrawal Event)

The neutronics report indicates the maximum worth of the control rods in the LCC is $4.43 (for the regulating rod). Historical data indicates the greatest integral reactivity worth of any control rod since initial criticality was $4.50. Annual measurement of control rod speeds support evaluation of the maximum reactivity addition rate; control rod drive speeds over the 15 in. span are typically about ½ in. per second (30 in. per minute). A set of TRACE calculations was performed to simulate the effect of a continuous control rod withdrawal to the full out position for various integral control rod worths. Reactivity addition was modeled based on the fraction of total reactivity added as a function of position, and a constant speed was assumed to determine the fraction of the total integral reactivity added as a function of time for withdraw-intervals (full-in to full-out) of 5, 15, 30, 45, 75, 90, 120 and 135 seconds. Reactivity scale factors of $3, $4, $5, $6 and $7 were applied to each interval to calculate average fuel element response to the transient. The time dependent power resulting from this set of calculations was modified with the hot channel peaking factor to simulate the LCC hot channel, and a time dependent power calculation was performed. The characteristic of a 5 second interval are essentially a reactor pulse with a small perturbation on the pulse-tail.

The CHFR (using the Bernath correlation) was calculated as a minimum of 2.41 for the $7 reactivity additions to a minimum of 5.76 for a $3 addition, both at 135 seconds (2.25 minutes) for full reactivity addition. Power, temperature, and reactivity characteristics for a reactivity addition to $3 over 45 seconds is displayed in Figs. 18 and 19.

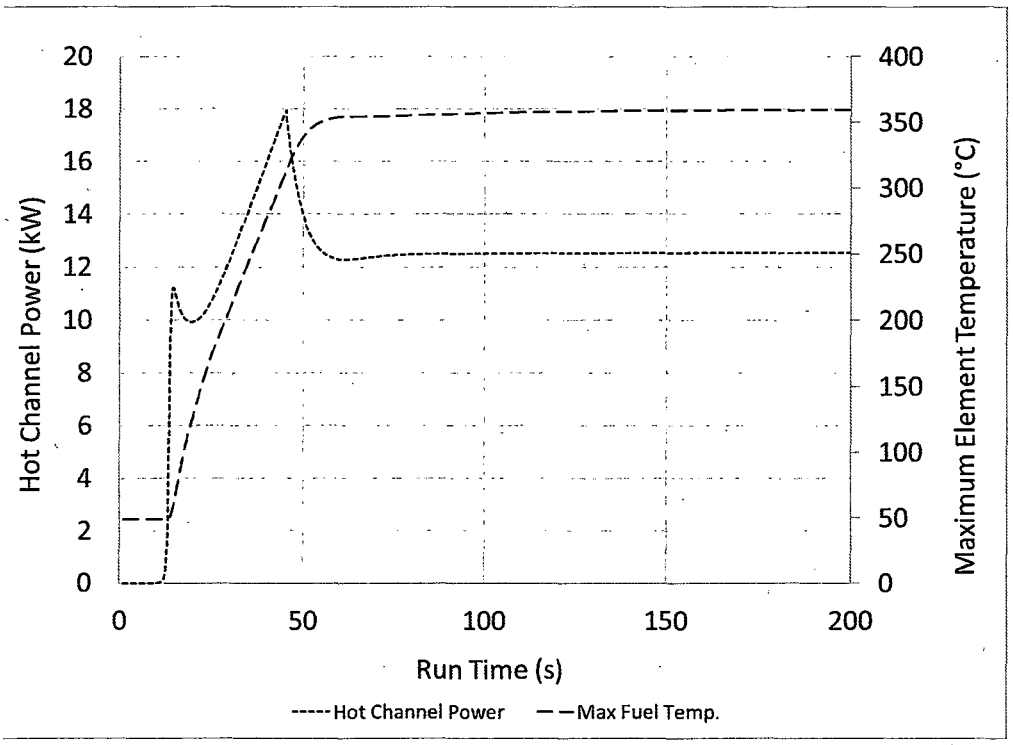

Figure 18: Hot Channel Power and Maximum Fuel Temperature Versus Run Time for a $3 Reactivity Addition in 45 Seconds

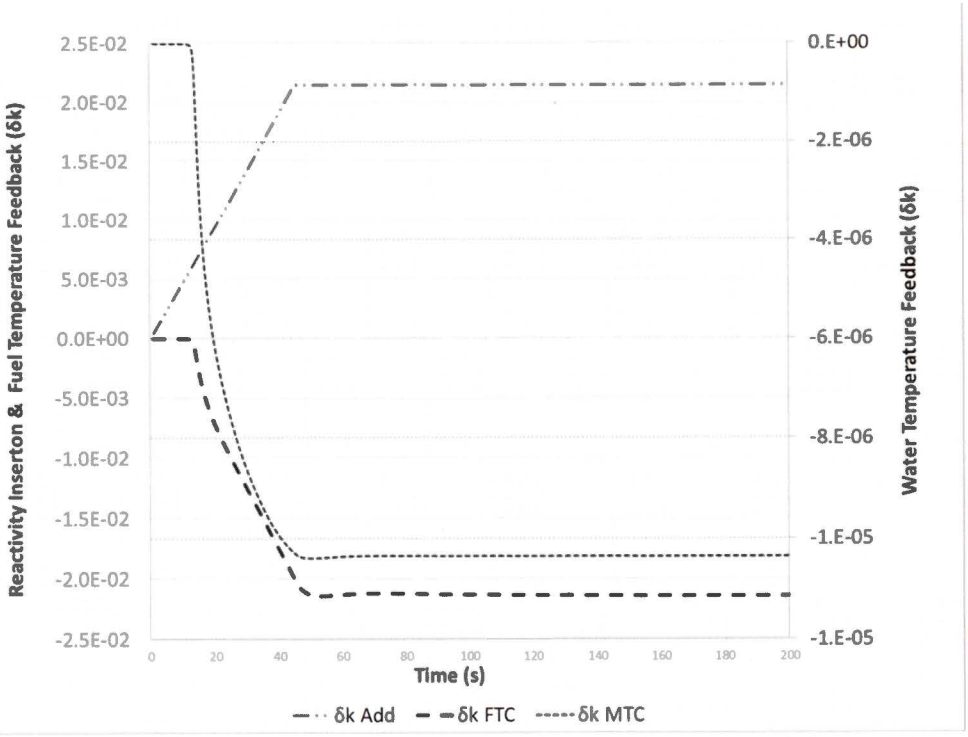

Figure 19: Reactivity Addition, Fuel Temperature Reactivity Feedback, and Moderator Temperature Reactivity Feedback Reactivity Versus Time for a Continuous Reactivity Addition for $3 in 45 Seconds

Power level response versus time is illustrated in Figs. 20 and 21 for $3 and $7 insertions that occur over a range of intervals.

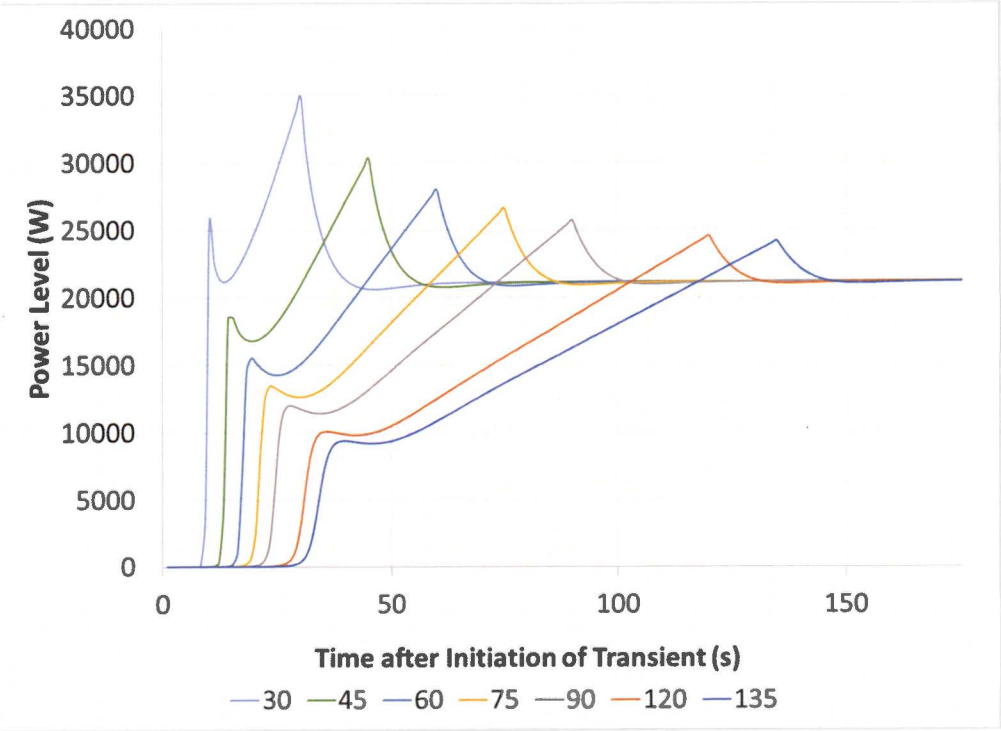

Figure 20: Power Level Versus Time After Initiation of Transient for a Continuous Rod Withdrawal of $3 in Reactivity

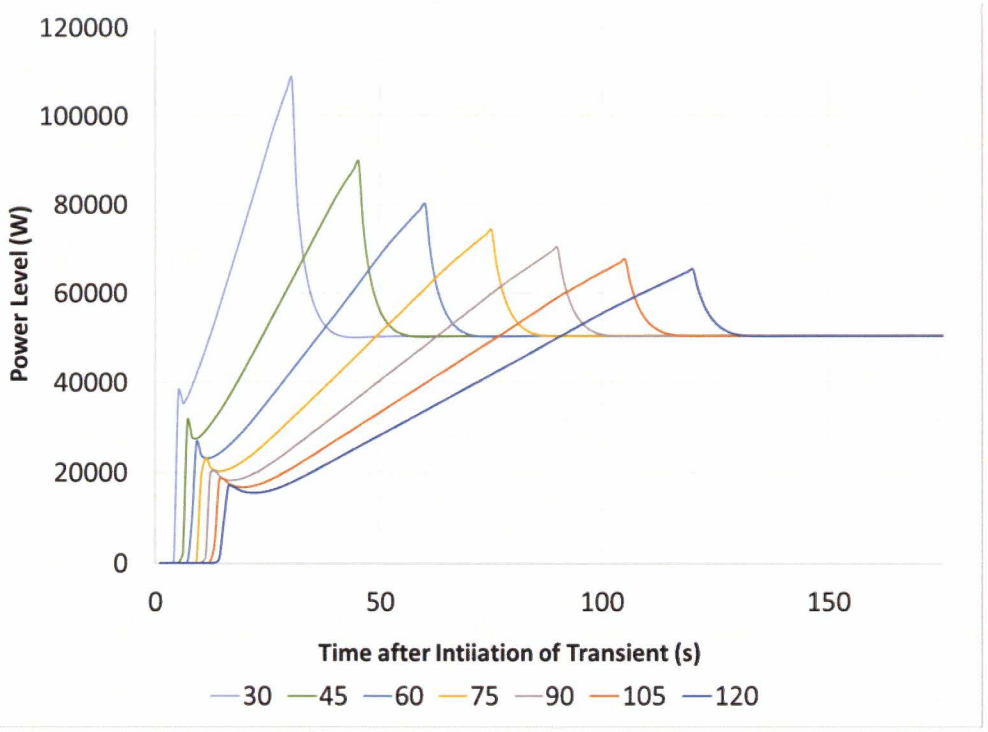

Figure 21: Power Level Versus Time After Initiation of Transient for a Continuous Rod Withdrawal of $7 in Reactivity

Notably, as the interval time for the reactivity addition increases, the maximum element power over the interval decreases. The element power level following the transient [Table 12, 'Element Power (kW)] is strictly a function of the total reactivity addition regardless of the reactivity insertion rate. The maximum fuel temperature resulting from specific reactivity additions occurs after the pulse as a function of the total reactivity added [Table 12, 'Peak Temp (°C)'] and therefore did not vary significantly with varying time intervals.

Table 12, Response to Reactivity Addition

Δk Addition	Peak Temp (°C)	Final Element Power (kW)
$1.00	226	7.15
$2.00	399	14.60
$3.00	572	21.21
$4.00	748	28.42
$4.75	835	33.99
$5.00	923	35.75
$6.00	1090	43.17
$7.00	1252	50.38

The maximum fuel temperature for the $5 reactivity addition approaches but does not exceed the 950°C fuel temperature safety limit. Maximum reactivity addition up to $4.75 results in a maximum fuel temperature 748°C, well below the fuel temperature safety limit, and is greater than the maximum control rod worth measured since initial criticality of the NETL.

Following a reactivity insertion transient with a total reactivity addition at $3 or less steady state power level

does not exceed 1.1 MW. If no credit taken for protective action from the power level instrumentation channels, power levels may exceed 1.1 MW during the transient, but total reactivity addition up to $5 does not exceed the fuel temperature safety limit and remains well within the minimum CHFR.

control rod drive systems at the UT TRIGA are independent and cannot be operated in a group. The control rod drives are controlled by software, and interlocks (including prevention of withdrawing multiple control rod simultaneously) are tested annually. The regulating rod and the two shim/safety rods are powered by stepper motors (with individual power supplies for each rod drive system) while the transient rod uses an analog motor. The regulating rod drive can be operated to automatically maintain a demand power level, the shim rod drives can only be operated manually. A failure mode that causes withdrawal of multiple control rods has not been identified. Continuous withdrawal of a single control rod with an integral worth less than $4.75 at any control rod drive speed is adequate to maintain fuel temperature less than the maximum fuel temperature limit with a 115°C margin.

4.4 LOCA Analysis

The LOCA analysis was a 2-step process with the first a steady-state TRACE calculation to establish initial conditions at 25 kW. This was followed by a TRACE restart case initiated as a transient calculation, with fission and fission product power decay in time established using the method of ANSI/ANS-5.1-2014, Decay Heat Power in Light Water Reactors (as described). Four cases were calculated (Table 13) using four intervals between shutdown and instantaneous replacement of water cooing with air cooling. The time-dependent behavior is shown in Fig. 22 over four hours following shutdown.

Table 13: LOSS OF WATER-COOLING ANALYSIS

DELAY FOR AIR COOLING (s)	MAXIMUM TEMPERATURE (°C)
1	709
60	699
600	663
1200	637

In a rational scenario, an automatic shutdown will be initiated before the core is voided by a low pool water level trip. Drain down of pool water under the most exaggerated conditions will require on the order of 10 to 20 minutes before water is voided from the core area. A 10-minute delay will result in a maximum temperature of 663°C, and a 20-minute delay will result in a maximum temperature of 637°C.

There are other practical considerations not considered in modeling that make the analysis conservative in a LOCA event. A drain-down through the beam ports (the only path for flow) will not drain below the core, and some lower portion of the fuel elements will remain in a water environment to provide heat removal with conduction through the stainless-steel cladding. The air cooling will occur in extremely humid conditions, increasing heat removal capability.

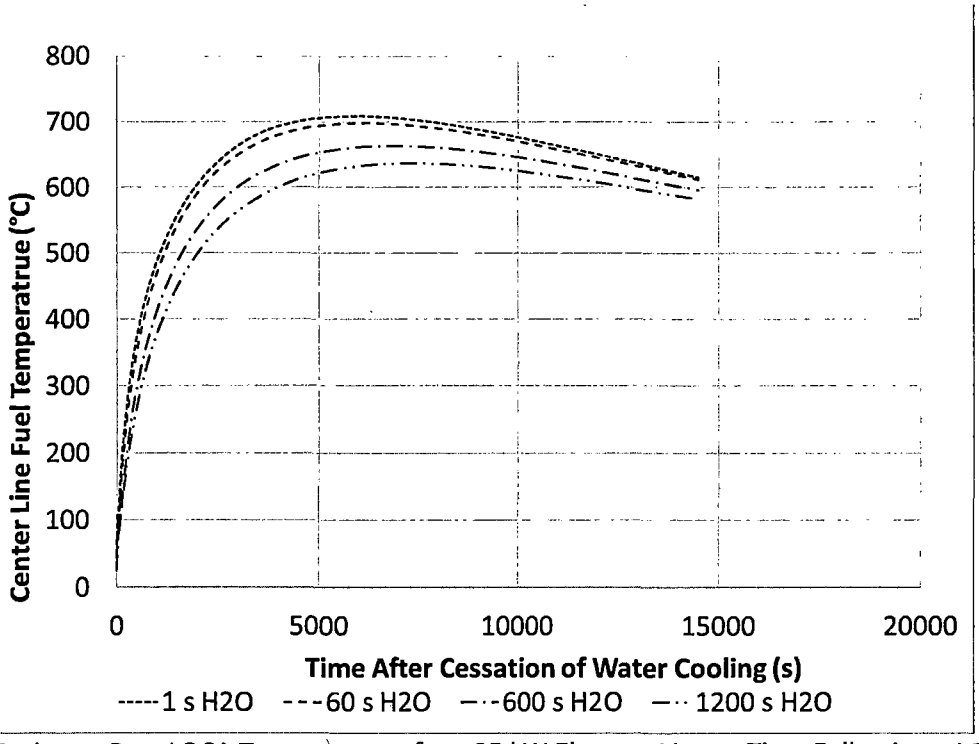

Figure 22: Maximum Post LOCA Temperatures for a 25 kW Element Versus Time Following a LOCA Event (shown for a variety of delay times for air cooling)

The UT TRIGA LCC hot channel fuel element temperature during a LOCA is calculated to rise to 709°C (assuming a minimal 1 second delay between reactor shutdown and displacement of water with air). Analysis of fuel performance during a LOCA for the AFFRI reactor predicated on 72 hours of full power per week indicates a maximum fuel temperature of about 550°C if there is no delay before water displacement and about 475°C assuming a 15-minute delay. The UT analysis assumes equilibrium steady state analysis, about 2.3 times the power history of the AFFRI reactor, generating more decay heat.

The maximum temperature of 709°C provides a margin of 241°C to the limiting temperature. Therefore, the LCC is adequate maintain fuel integrity unchallenged by temperature in a LOCA.

5.0 SUMMARY AND CONCLUSION

There are two limits that ensure TRIGA fuel integrity during steady-state operations and one for pulsing. During steady-state operations a fuel temperature limit of 950°C and a CHFR limit of 2.0 applies. During pulsing operations, a fuel temperature limit of 830°C applies. Thermal-hydraulic calculations using TRACE linked to a neutronics calculation (using MCNP 6.2) was performed to available safety margins in operation of the UT TRIGA reactor LCC.

With the hot channel of the UT LCC producing 24.3 kW, analysis shows that the CHFR is greater than 4.0 with a maximum fuel temperature of 650°C. Therefore, steady-state operations at 1.21 MW with the LCC is adequate to assure the safety limit is met.

In pulsing operations to $3 from non-power conditions, the maximum fuel temperature is calculated to be 378°C. Pulsing at power from the maximum power level (reserving $3 for the maximum pulse), fuel temperature is calculated to be 579°C. These temperatures are well below the temperature limit for pulsing operations. Therefore, a $3 pulsing limit is adequate to assure the safety limit is met for the LCC.

The maximum fuel temperature from a continuous reactivity addition event up to $4.75 at any reactivity addition rate will not exceed 835°C. The control rod drive system limits reactivity addition by multiple control rods. Therefore, limiting each integral control rod worth to less than $4.75 is adequate to assure the fuel temperature to the safety limit is met in a continuous rod withdrawal event for the LCC.

A loss of coolant accident after continuous full power operations to steady-state conditions will not result in fuel temperature greater than 709°C (with the cooling delayed by 1 second). Therefore, 1.21 MW operations with the LCC ensures cooling is adequate for fuel integrity in a loss of coolant accident.